Utah State University
DigitalCommons@USU

All Graduate Plan B and other Reports | Graduate Studies

5-2009

Investigations into mapping lava flows in the Snake River Plain, Idaho

Vinita Ruth Hobson-Broko

Follow this and additional works at: https://digitalcommons.usu.edu/gradreports

 Part of the Geology Commons

Recommended Citation

Hobson-Broko, Vinita Ruth, "Investigations into mapping lava flows in the Snake River Plain, Idaho" (2009). *All Graduate Plan B and other Reports*. 1099.
https://digitalcommons.usu.edu/gradreports/1099

This Report is brought to you for free and open access by the Graduate Studies at DigitalCommons@USU. It has been accepted for inclusion in All Graduate Plan B and other Reports by an authorized administrator of DigitalCommons@USU. For more information, please contact rebecca.nelson@usu.edu.



Investigations into mapping lava flows in the Snake River Plain, Idaho

by

Vinita Ruth Hobson-Broko

A report submitted in partial fulfillment of
the requirements for the degree

Master of Science

in

Applied Environmental Geoscience

UTAH STATE UNIVERSITY
Logan, Utah

2009

Table of Contents

Abstract 3

Introduction 4

Geologic Setting 5

Formation of the Snake River Plain 10

Plume (Hotspot) theory 10

Non-Plume theories 13

Summary of Theories 15

Mapping Lava Flows at Craters of the Moon using Landsat ETM 16

Methods 18

Supervised Classification 18

Unsupervised Classification 24

Principal Component Analysis 42

Results 48

Field Mapping Twin Falls NE, Hunt, and Eden NE Quadrangles 56

Methods 56

Results 63

Conclusions 67

References 68

Abstract

The origin of the Snake River plain continues to be debated, but the plume model is most popular at the current time. Some theories, such as meteorite impact, have been excluded, but the remaining theories require more scrutiny.

Various methods of examining phenomena in the Snake River Plain were employed. Unsupervised classification of Landsat ETM data indicates that spectra can be used to differentiate between flows. However, photographs of flows at Craters of the Moon National Monument show wide variations in texture and color within a single flow. Vegetation grows preferentially on the smoother pahoehoe slabs and significantly impacting the spectra observed through remote sensing. Additional vegetation would prohibit using Landsat ETM to map lava flows reliably. Landsat ETM is not a viable method to map the lava flows in quadrangles Twin Falls NE, Hunt, and Eden NE, since they have significantly more loess and vegetative cover.

Elevation data reveal the locations of the ramparts at the source vent, but do not define the edge of a flow except when an inflated lobe terminates the flow. Field observations of terrain and geochemical analysis of samples defines the flows and their source vent.

Introduction

Volcanic activity occurs in many regions on Earth, many of them very remote. Volcanoes and flows close to populated centers have been studied in varying degree, but remote volcanics remain largely unstudied. By using satellites and other remote sensing methods, information about the eruptive history can be derived and potentially, the hazard these remote volcanic areas may pose to current and future generations can be estimated. Furthermore, developing a method to characterize the chemical and temporal aspects of terrestrial volcanics is a necessary step toward studying volcanics on other planetary bodies. Earth scientists can familiarize themselves with an area beginning fieldwork by using remotely sensed data and derived information.

Any method must first be developed using an area for which ground truth is available or can be collected. The Craters of the Moon (COM) lava field in the Snake River Plain (SRP) contains flows and cinder cones that can be used to develop such a method. Establishing a time order is an essential part of understanding events that formed the SRP. To develop a timeline of events for an eruptive center, the individual flows must be distinguished. Spectral data from satellite-borne sensors such as Landsat ETM can be used to differentiate the volcanic units in the COM lava field. Examining spectral characteristics

will give clues to the chemical composition, flow features, and any obscuring phenomena (loess, etc). Fieldwork will provide the ground truth necessary to have confidence in the remote sensing results.

After discovering that vegetation and weathering had the most effect of the spectra, using remote sensing to differentiate between flows near Twin Falls was determined to be an unreliable method. Twin Falls and its surrounding area has more loess covering the lava flows and more vegetation, including irrigated agricultural fields. A more conventional approach to mapping these flows had to be used. Aerial photographs and fieldwork on the ground were used as the primary data and remotely sensed data became secondary.

Geologic Setting

The Snake River Plain (SRP) is an arc-shaped valley in Idaho that is filled with volcanic deposits (Figure 1). Bounded by basin and range phenomena to the north and south, the SRP is nearly flat by comparison (Figure 2). The valley floor is filled with rhyolitic deposits and capped with thin basaltic flows, some of which are quite young (2-15 Ka) (Kuntz, 1988). Most of the basalt effused from small shield volcanoes and fissures. Occasional cinder cones and phreatic phenomena contribute to the unique character of the SRP. Calderas in the Eastern Snake River Plain have been found to increase in age from 2 Ma at Yellowstone to 16 Ma at the Nevada-Oregon-Idaho border

(Figure 3). Evidence for some of the calderas that erupted the thick sequences of rhyolite can be found near the edges of the SRP (Hackett and Bonnichsen, 1994). Below the surface, a 45 km-wide sill-like feature extends beneath the eastern SRP (Peng and Humphreys, 1998). The Snake River flows along the southern edge of the plain, cutting through layer upon layer of basalt, rhyolite, and ash. Volcanic features dot the plain that are much younger than expected from a hotspot.

Figure 1: Regional Geologic Categories modified *from* http://volcano.und.nodak.edu/vwdocs/volc_images/north_america/yellowstone.html

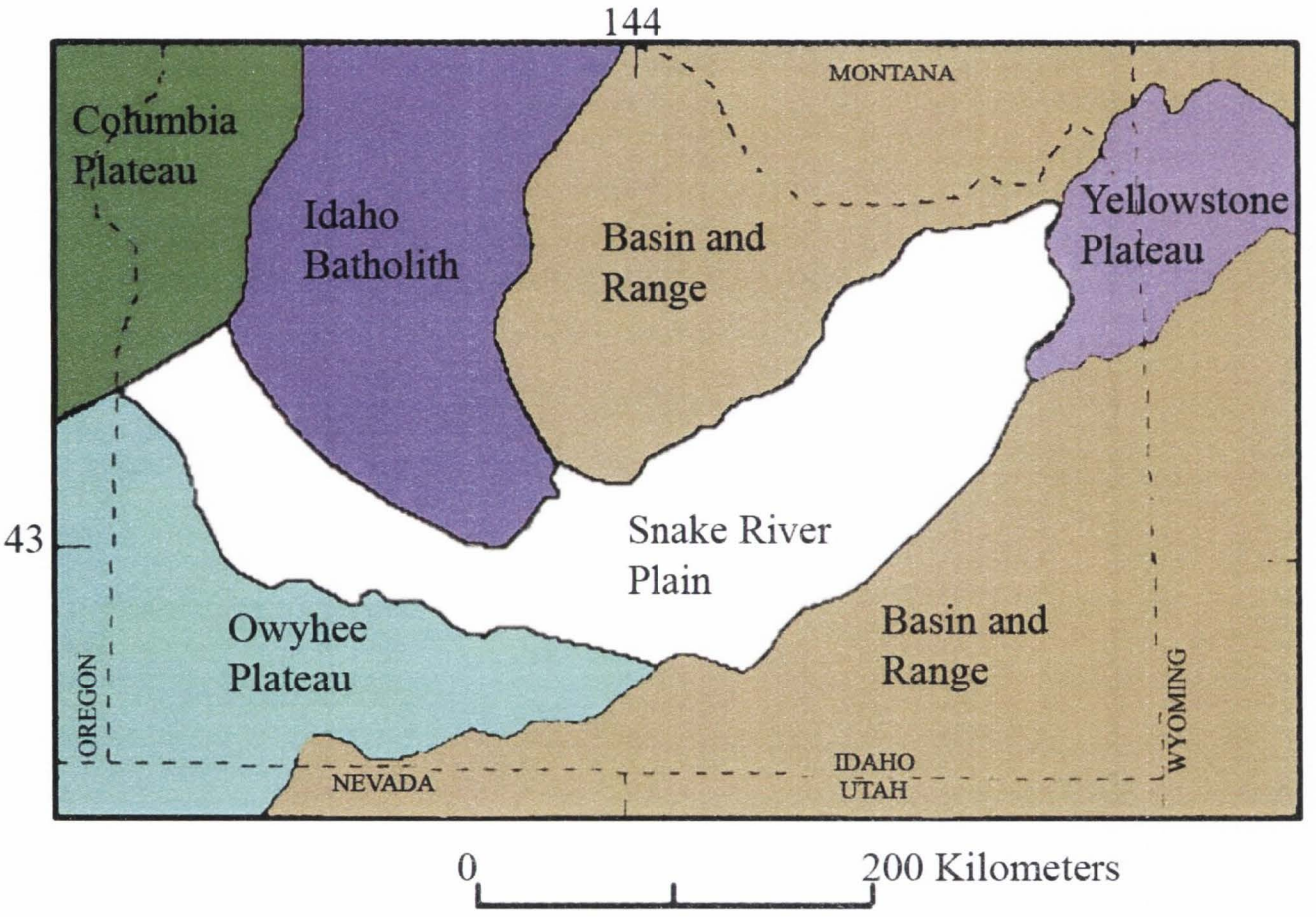


Figure 2: Digital Elevation Model *from*
http://volcano.und.nodak.edu/vwdocs/volc_images/north_america/yellowstone.html

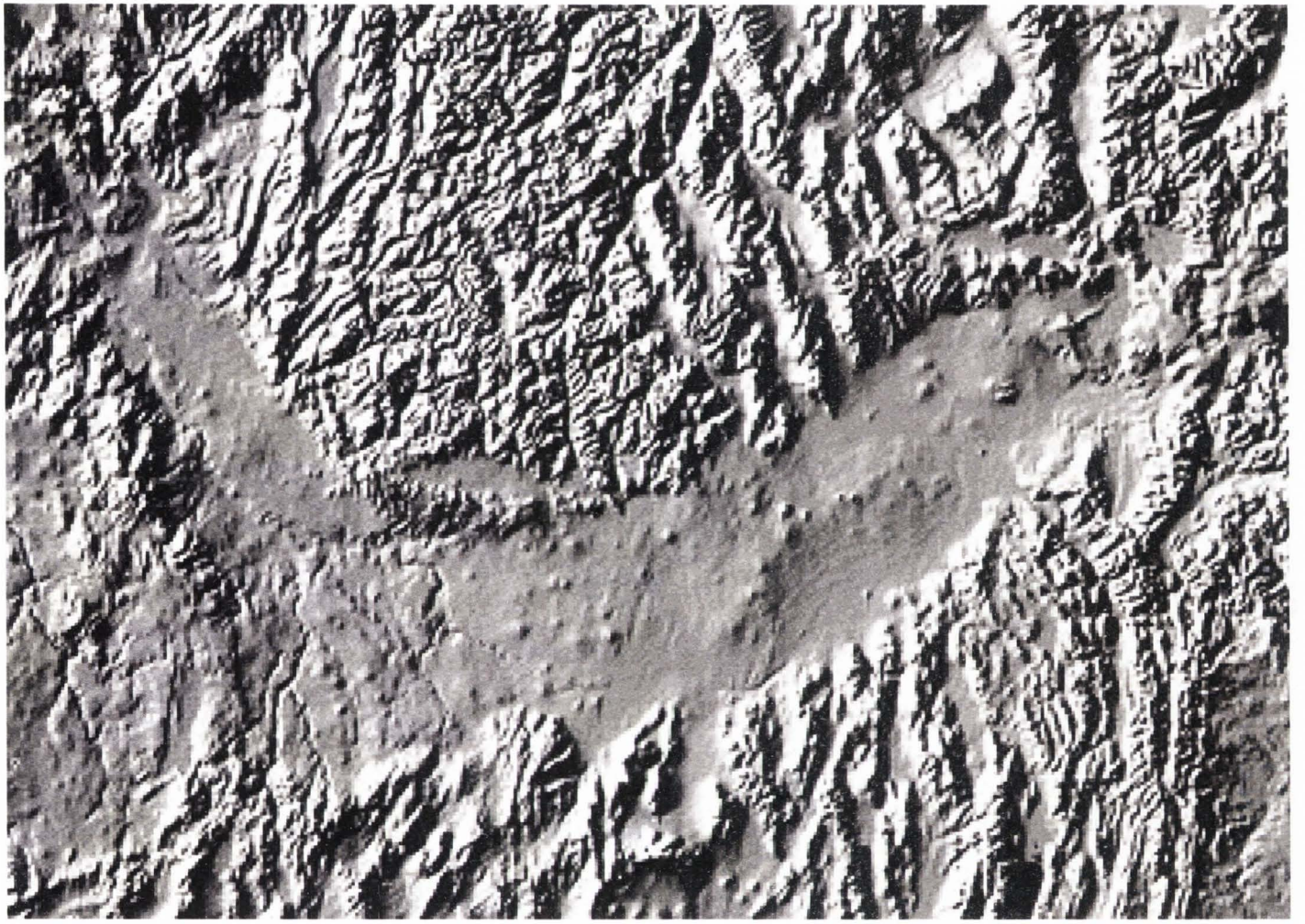
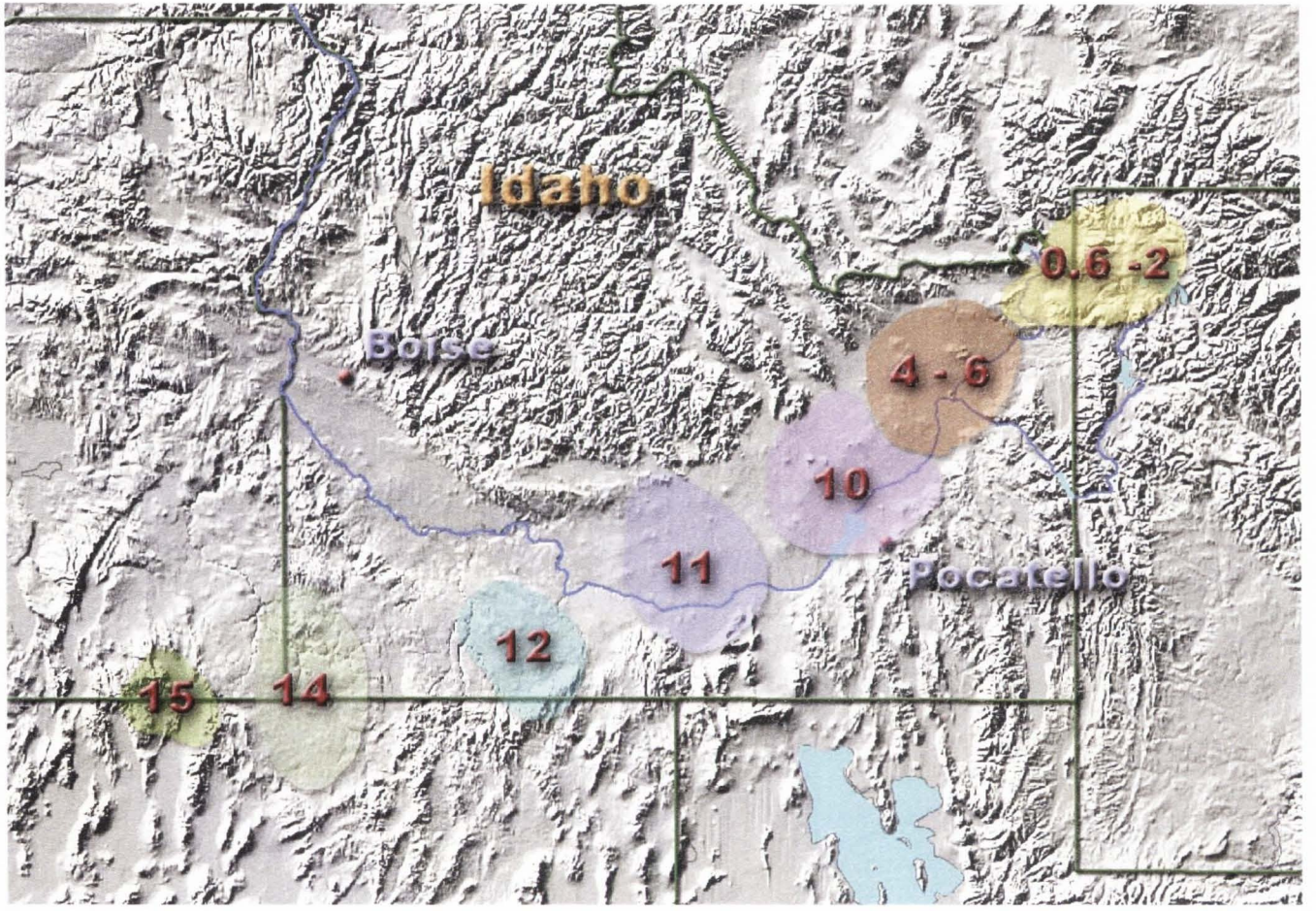


Figure 3: Calderas increase in age away from Yellowstone location *from* http://en.wikipedia.org/wiki/Image:HotspotsSRP.jpg



Formation of the Snake River Plain

Several theories have been proposed for the origin of this uncommon area. The most popular theory, a mantle plume, is commonly referred to as the hotspot theory. Several non-plume theories have been suggested, including one that alleges the phenomena can be explained by shallow melting in the mantle.

Plume (Hotspot) theory

Bounded by Basin and Range phenomena to the north and south (Figure 1), the Snake River Plain is believed by many to be the result of a hot spot that currently sits beneath Yellowstone National Park. As the continental plate moves over this hotspot, the trail left behind the location of the hotspot subsides, leaving a topographic low (Figure 2).

Hotspots are commonly associated with buoyant mantle material that rises toward Earth's surface, causing topographic uplift above it (Hill, 1991). Buoyancy is a function of density – affected by both temperature and composition. The plume consists of material that is less dense than the surrounding mantle. The temperature of the plume material can be the same as the surrounding material if the density is lower. The composition can be the same if the temperature is higher. The combination of small differences in composition and small differences in temperature could provide enough buoyancy to bring the

material to the surface. As the plume rises, the leading edge encounters resistance from the mantle material above. The uppermost portion slows, but the following material continues to rise, accumulating a "head". The head circulates its material, reducing the friction of interacting with neighboring material on its upward migration. During this process, mantle material along the route becomes entrained in the plume head, affecting its size, temperature and/or composition. As the plume rises through the Earth, pressure drops continuously (less and less material overlying the plume). With this decompression, melting of the mantle material can begin.

As the plume intersects the lithosphere, the partially molten head flattens against the harder, cohesive mass, searching for a passage to continue its upward movement. The upward flow continues through the plume tail, collecting hot mantle material against the lithosphere, raising its temperature. As mafic magmas intrude the crust, the crustal material can begin to melt and join the plume head material, producing rhyolitic volcanism, followed by basaltic extrusion. Alternately, the lithosphere and crust may be rifted apart to provide the basaltic plume material an escape route. All the while, the continental plate is moving over the plume, dragging the effects of the plume away from the point of intersection.

The topographic high surrounding Yellowstone, combined with regions of faulting and seismic activity that propagate in a widening arc away from Yellowstone, indicate the North American plate is moving southwest over a stationary source of heat and buoyancy (Pierce and Morgan, 1992). As the plate moves away from the plume source, the 9 km-thick sill of basaltic material is emplaced in the mid-crust.

To account for the location of the Columbia River Basalts, Geist and Richards (1993) suggest a modification of this theory. It is also possible that the plume head did not intersect the North American plate directly. Instead of the plume head intersecting the North American plate, it may have intersected the Farallon plate. The existing plume would have been dragged beneath the North American by the subducting Farallon plate while shielding the continent from the effects of the plume tail. Eventually the plume contributed to the break off of the slab, allowing the rising mantle material to escape from beneath the slab and intersect the surface. The accumulated mass of material rose from its deflected position to erupt the Columbia River Flood basalts. The plume tail recovered to a vertical position and began the eastern SRP-Yellowstone path.

Camp (1995) asserts that the preexisting Precambrian margin of the continent is responsible for the emplacement of basalts away from

the current hotspot track. The rapidly accumulating, buoyant mantle material sought the thinnest crust, finding it where oceanic terranes were accreting adjacent to the thick, cold Precambrian craton. Decompression melting and mixing with the craton accounted for variations in chemical composition.

Non-Plume theories

If there were a mantle plume feeding the Yellowstone hotspot, there should be a broad, shallow region of slow mantle velocity (Saltzer and Humphreys 1997). However, seismic tomography reveals a narrow, deep feature (Saltzer and Humphreys 1997, Humphreys et al. 2000, Christiansen et al. 2002). A different theory has been proposed – shallow mantle melting. If mantle partially melts, erupting the melt onto the surface, the rest of the mantle material (residuum) must go somewhere for eruptions to continue. The melting mantle would be more buoyant than the residuum, causing convection. Convecting the residuum to the side of a phenomenon slowly propagating northeast would result in a "hotspot" track with slow seismic features in the center of the propagation path where the partial melting occurs and faster seismic characteristics in the denser residuum. While the data fits the model, the question of how to start the phenomenon remains.

Christiansen et al. (2002) propose that the collision of the Pacific and North American plates resulted in back-arc lithospheric thinning which caused upwelling and widespread partial melting of mantle. The phenomena would propagate along an axis. One direction led to Yellowstone, the other toward Newberry. However, the two arms lie at an angle to each other, cause unknown. Humphreys et al. (2000) suggest that the melting was triggered by the subduction of the Farallon and Juan de Fuca plates. The subducting plate motion sets up a convection cell that forces mantle material up to the base of the crust. Because of the angle at which the Farallon/Juan de Fuca plate was subducted, the surface expression of the hotspot would begin in the center and propagate northeast toward Yellowstone and northwest toward Newberry. The difference in this hypothesis is that the residuum is left in the track; new mantle must flow past the residuum to reach the current surface expression.

Other non-plume theories discussed by Pierce and Morgan (1992) include an eastward propagating rift, a transform boundary zone, and crustal flaws. If the SRP were an eastward propagating rift, the direction of extension should be perpendicular to the rift axis. The faults in the area do not support this theory. A transform boundary zone at the north end of the Great Basin implies that the magnitude of basin and range extension north of the SRP would not be comparable

with the activity to the south. The 1983 Borah Peak earthquake supplied evidence that the extension north of the plain is similar in magnitude to the extension in the Great Basin. A transform fault is not necessary to balance the extension rates. A crustal flaw should show a weakness beyond the surface expression of the SRP/Yellowstone track, but none has been found northeast of Yellowstone.

Summary of Theories

Scientists continue to gather data and propose modifications of theories, but the plume model is most popular at the current time. Some theories, such as meteorite impact, have been excluded, but the remaining theories require more scrutiny. The plume theory does not account for the location of the Columbia River Basalts and therefore does not provide a location for the large volumes of plume head material that should have erupted at the start of the hotspot track. Shallow melting is supported by one tomographic study (Christiansen, 2002), but another is inconclusive (Saltzer and Humphreys, 1997).

Mapping Lava Flows at Craters of the Moon using Landsat ETM

Some lava flows occur in remote locations where field investigation is difficult or impossible. In order to develop a method to conduct investigations without first-hand information such as ground truth, methods must first be tested and refined extensively with data from regions for which ground truth is available or can be acquired. The geochemistry and flow features of the lava flows at Craters of the Moon National Monument and Preserve (CNMP) have been studied in detail, but fewer studies from satellite data have been conducted. Lefebvre (1975) studied Landsat 1 MSS data from bands 4 through 7 (equivalent to Landsat TM bands 1 through 4, Table 1) and with the addition of aerial photography and field investigation, determined that the outer boundary of the young flows could be identified, that a'a flows had a lower radiance than pahoehoe flows, and the glassy crust of flows like the Blue Dragon flow reduces the radiance observed in the bands studied.

Table 1: Spectral range of bands and spatial resolution for the ETM sensor

	Wavelength Range (micrometers)	Spatial Resolution (Meters)	
Band 1	0.45 - 0.52	30	Blue
Band 2	0.52 - 0.60	30	Green
Band 3	0.63 - 0.69	30	Red
Band 4	0.76 - 0.90	30	Near Infrared
Band 5	1.55 - 1.75	30	Mid-Infrared
Band 6	10.40 - 12.50	60	Thermal Infrared
Band 7	2.08 - 2.35	30	Mid-Infrared
Band 8	0.52 – 0.90	15	Panchromatic

Young lava flows at CNMP were selected to test methods for remote mapping of recent volcanics. These late Pleistocene to Holocene basalt flows have been mapped to 1:100,000 scale (Kuntz et al., 1988) and have only minor vegetative cover. Major flow units can be distinguished from each other using unsupervised classification of Landsat TM bands 1 through 7, but differentiation of flows within these units presents greater difficulty. Principal component analyses revealed that during the daytime, thermal infrared variations outweigh variations in all other bands. Larger-scale features were observed like edge effects attributable to changes in surface roughness or texture that might occur at flow fronts or at boundaries between flows. Several

flows were selected for further examination in the field, based on accessibility and scientific interest.

Craters of the Moon lava field is a geologically young series of lava flows in the Snake River Plain erupted in 8 distinct periods (Kuntz, 1982). Along with the Wapi and King's Bowl lava flows, Craters of the Moon lies along the Great Rift. The Great Rift is an 85 km long, 2-8 km wide belt of shield volcanoes, cinder cones, fissures and associated lava flows. Located within 42.5-43.5 N, 113-114 W, Craters of the Moon is the largest Holocene lava flow in the conterminous US. Because of the arid climate, the basaltic lava flows of the SRP do not degrade into soil as quickly as flows in wetter areas like Hawaii or the Galapagos archipelago. Radiocarbon tests have determined ages of 2000 to 15000 years (Kuntz et al., 1982), yet the flows retain character similar to Hawaiian flows that are several hundred years old. Many of the flows of the most recent eruptive period are almost devoid of vegetation. The older of these very young flows support vegetation where loess has settled in crevices and depressions.

Methods

Supervised Classification

A supervised classification is when the analyst selects pixels for several categories (pixels known to be of a certain origin or land

cover), then averages the values from each band to build a spectral profile and the remainder of the image pixels are sorted into the closest matching category. The purpose in this project was to isolate the basalt from the surrounding dirt-covered and vegetated area, so the variations within the lava flows would be observable. Vegetation displayed a much greater range of values in all bands and obscured the values of interest over the lava flows.

A supervised classification of a subset, cloud-free Landsat TM scene (Figure 4) resulted in 3 categories: loess-covered basalt, vegetation, and uncovered basalt (Figure 5). The supervised classification was based on a minimum of 20 samples per category which where compiled into one signature each. A minimum distance to means method was employed to assign categories. There were some errors of omission (areas interior to the lava flow were misidentified as loess-covered basalt) and errors of commission (north slopes in the mountain range were identified as basalt). To eliminate some of these errors, the basalt class was smoothed and a minimum number of contiguous pixels required. The resulting basalt/non-basalt mask (Figure 6) was applied to the original TM scene, leaving only data for the region of interest (Figure 7).

Figure 4: Cloud-free Landsat TM Scene used to isolate the Craters of the Mon lava flows from the surrounding vegetated areas

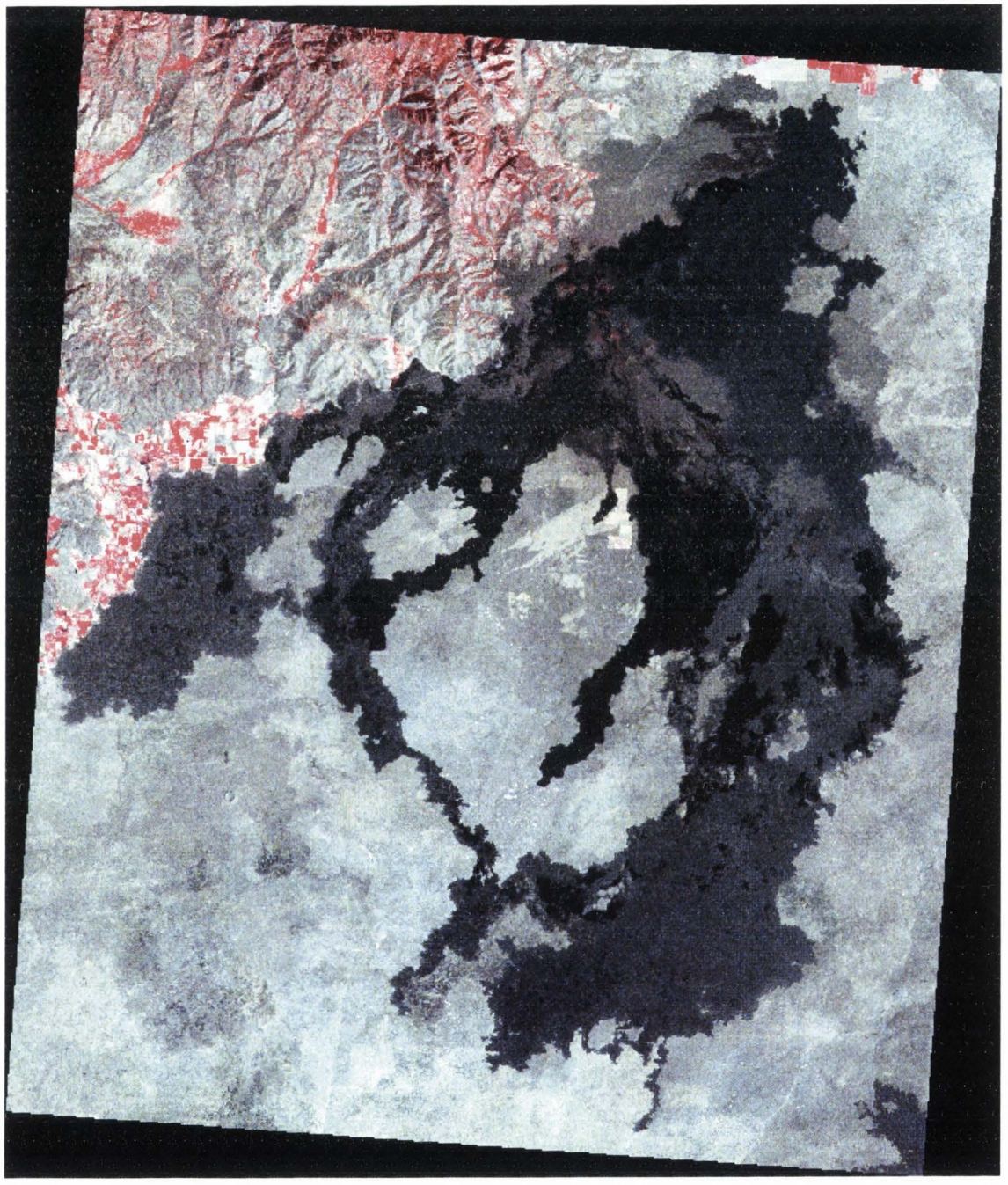


Figure 5: Supervised Classes from Landsat ETM Scene (Loess, Vegetation, Basalt)



Figure 6: Basalt/Non-basalt Mask derived from Landsat ETM Scene

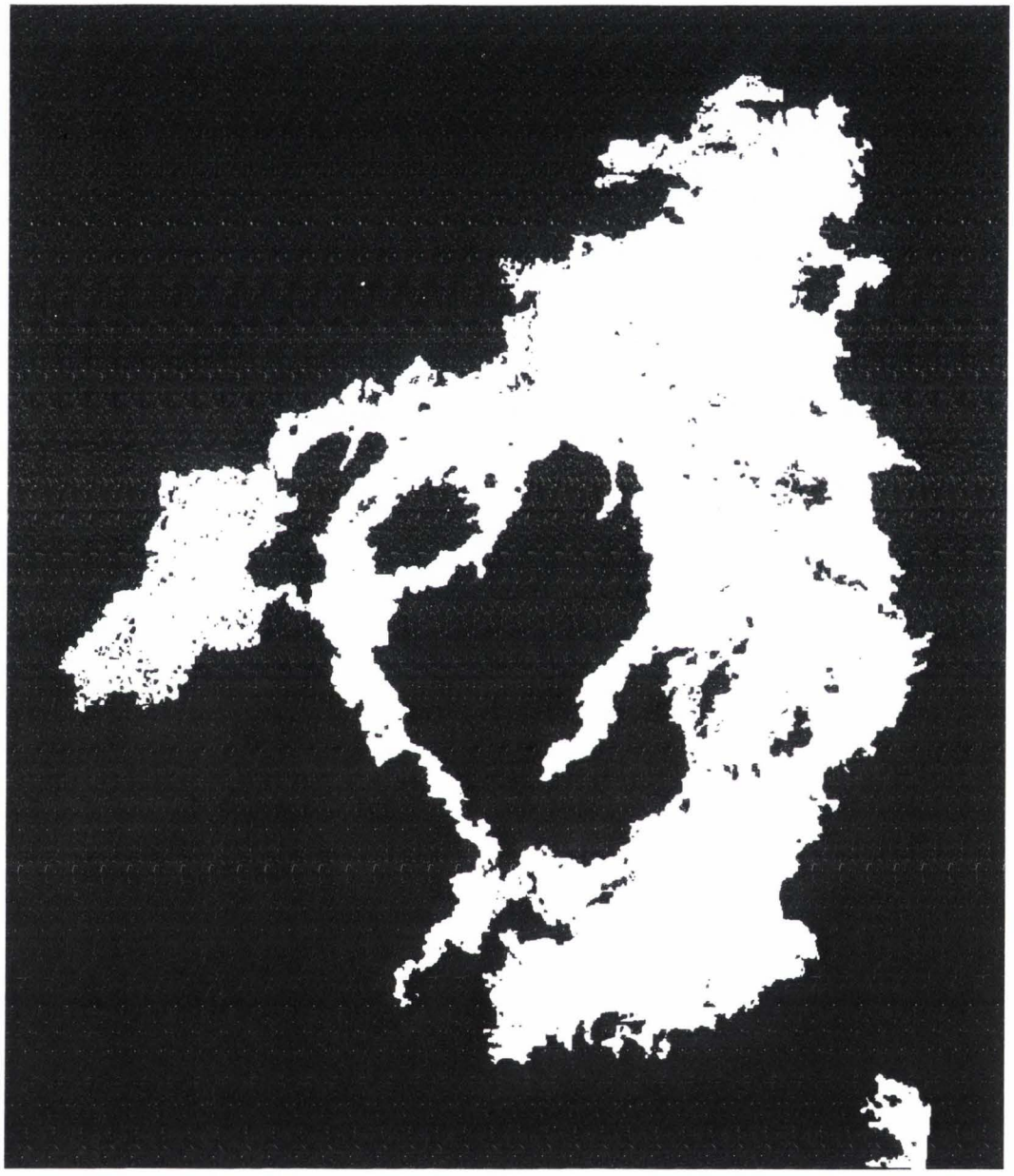
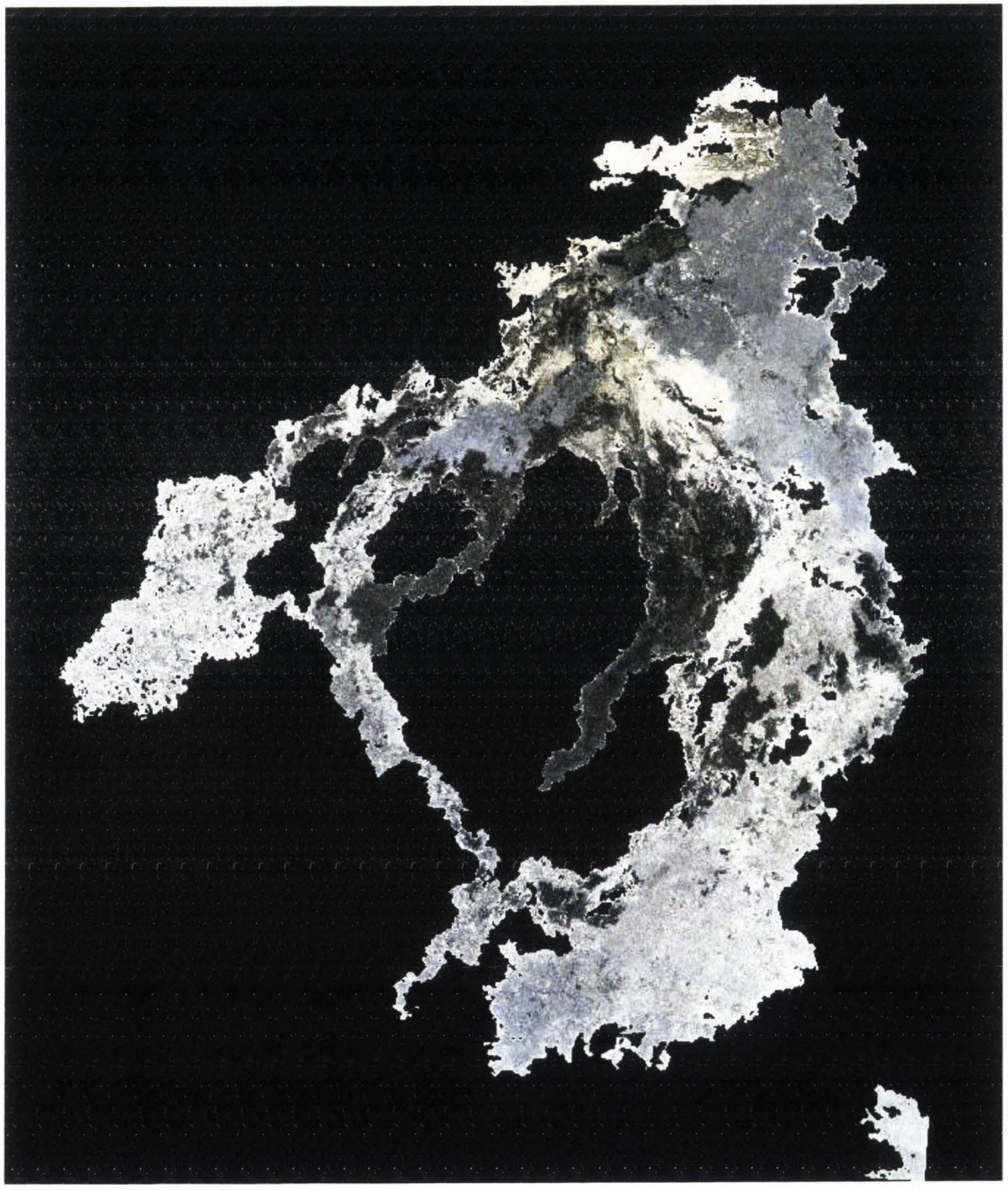


Figure 7: Isolated Basalt from Landsat ETM scene



Unsupervised Classification

An unsupervised classification allows the pixels to be separated by the computer algorithm into a selected number of categories. This method allows the discovery of differences between similar land cover types when the nature of the differences is not known prior to analysis.

It was anticipated that each flow would be distinguishable from the others, but the unsupervised classification (Figure 8) did not show an immediate identification of the individual flows. Overlaying a preliminary digitized version of the geologic map (Kuntz et al., 1988; shape file courtesy of National Parks Service) shows that the unsupervised classification does indicate that the spectra are related to the chemical components of the flows. The major chemical components of flows from CNMP are listed in Table 2 (Kuntz et al., 1992). While some flow trends can be inferred from the classification, it is not conclusive. Examining each band individually, a significant difference between one flow and the others is evident in the thermal infrared band. This response in the thermal band may be attributable to differences between flows in the amount of vessiculation (gas bubbles trapped in the upper part of the flow) discussed by Schaber (1973). However, larger-scale textures (a'a versus pahoehoe) were observed and may a larger role than vessiculation.

Figure 8: Unsupervised Classification of Isolated Basalt (10 classes), overlay of flow boundaries (Kuntz et al., 1998)

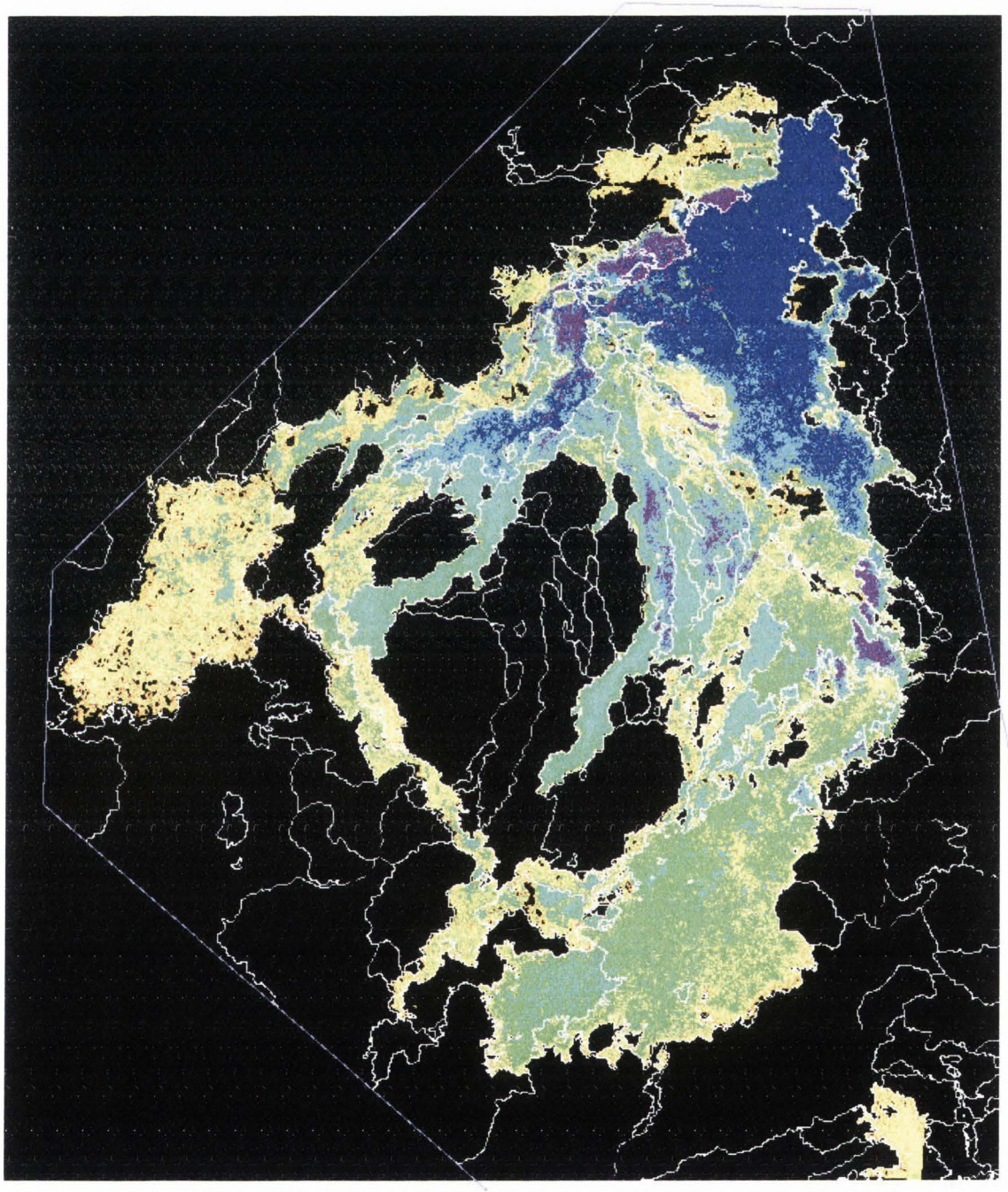


Table 2: Geochemical Analyses of Craters of the Moon lava flows in order of eruption (Kunz et al., 1992)

Eruptive Period	H	G	G	G	F	F	E	E
		Lava			Bottleneck		Lava	Grassy
Flow	Kimama	Creek	Sunset	Carey	Lake	Pronghorn	Point	Cone
Age (ka)	15.1	12.8	12.0	12.0	11.0	10.2	7.8	7.3
Sample No.	79K99	79K85	78K184	78K61	78K72	78K73	78K68	78K183
Major Oxides								
(percent)								
SiO2	45.24	43.50	49.65	47.22	46.58	45.52	45.64	47.25
TiO2	3.28	3.83	2.44	3.09	3.33	3.20	3.63	3.23
Al2O3	14.23	14.20	14.50	13.46	13.42	13.81	13.39	12.49
Fe2O3	1.27	2.16	4.53	0.89	1.35	1.20	1.79	8.62
FeO	15.11	14.78	10.47	14.93	14.71	14.96	14.28	7.45
MnO	0.28	0.27	0.24	0.26	0.27	0.24	0.23	0.25
MgO	4.53	5.21	3.14	3.91	4.21	4.10	4.67	3.82
CaO	7.50	8.13	6.47	8.24	8.78	7.48	8.18	8.40
Na2O	3.50	3.47	4.50	3.47	3.39	4.02	3.55	3.07
K2O	1.75	1.60	2.35	1.94	1.83	1.92	1.65	1.82
H2O+	0.33	0.38	0.12	0.24	0.23	0.32	0.37	0.19
H2O-	0.08	0.08	0.16	0.10	0.06	0.09	0.11	0.05
P2O5	2.64	2.78	1.56	2.29	2.46	2.18	2.13	2.33
Total	99.74	100.39	100.13	100.04	100.62	99.04	99.62	98.97

Eruptive Period	D	D	D	C	C	C	C	C
Flow	Little Park	Carey Kipuka	Silent Cone	Sentinel	Fissure Butte	Sheep Trail	Sawtooth	Indian Wells N.
Age (ka)	6.5	6.6	6.5	6.0	6.0	6.0	6.0	6.0
Sample No.	78K65	78K147A	78K15X	78K118	78K129	78K92	78K67	78K95A
Major Oxides (percent)								
SiO2	49.46	50.54	52.78	44.65	49.58	44.33	55.37	57.20
TiO2	2.55	2.42	1.86	3.70	2.41	3.65	1.70	1.29
Al2O3	14.28	14.16	14.06	12.97	14.40	13.77	14.67	15.11
Fe2O3	1.14	1.22	0.78	1.70	16.24	5.06	1.55	1.04
FeO	13.55	13.18	11.55	14.55	0.02	11.31	11.21	10.23
MnO	0.24	0.22	0.22	0.27	0.25	0.25	0.20	0.21
MgO	3.08	2.95	1.90	4.90	2.82	5.57	1.94	1.45
CaO	6.49	6.28	5.39	9.60	6.36	8.33	4.95	4.12
Na2O	4.28	4.28	3.51	3.04	3.86	3.36	4.12	3.97
K2O	2.30	2.38	2.71	1.56	2.26	1.50	3.04	3.40
H2O+	0.43	0.46	0.61	0.37	0.32	0.18	0.16	0.43
H2O-	0.14	0.15	0.16	0.06	0.17	0.08	0.04	0.10
P2O5	1.60	1.46	1.13	2.87	1.51	2.77	0.87	0.62
Total	99.54	99.70	96.66	100.24	100.20	100.16	99.82	99.17

Eruptive Period	B	B	A	A	A	A	A
		Devils			Big	Trench Mortar	Blue
Flow	Minidoka	Cauldron	Highway	Serrate	Craters	Flat	Dragon
Age (ka)	4.5	4.5	2.4	2.4	2.4	2.2	2.1
Sample No.	79K94	78K81	78K151	78K99	78K120	78K126	78K52
Major Oxides							
(percent)							
SiO2	48.40	48.73	62.88	59.91	52.04	51.08	49.01
TiO2	2.96	2.93	0.67	0.95	2.54	2.57	2.87
Al2O3	14.06	13.62	14.49	13.94	13.91	13.29	13.41
Fe2O3	1.09	1.35	0.88	2.94	1.33	1.72	0.77
FeO	14.44	13.90	7.58	7.44	13.40	12.16	14.50
MnO	0.26	0.22	0.17	0.18	0.24	0.23	0.24
MgO	3.83	3.54	0.27	0.52	2.68	3.05	3.34
CaO	6.92	7.12	2.94	3.55	6.76	6.82	6.93
Na2O	3.58	4.21	4.20	4.00	3.57	3.55	3.61
K2O	1.96	2.00	4.64	3.91	2.31	2.39	2.03
H2O+	0.26	0.23	0.14	0.11	0.18	0.13	0.20
H2O-	0.06	0.08	0.03	0.01	0.03	0.06	0.14
P2O5	2.12	1.88	0.14	0.29	1.47	1.44	1.77
Total	99.94	99.81	99.03	97.75	100.46	98.49	98.82

Photographs of the flows were taken at sites along the length of the flows. Dirt roads and jeep trails crisscross the BLM land surrounding the lava flows, allowing access to areas outside the developed Monument. The photographs show wide variations in texture within a single flow. The Grassy Flow (Figure 9-12) has areas of pahoehoe next to areas containing only small broken pieces of clinker. Closer to the vent source, a'a spires were observed, along with increasing amounts of red oxidation. Photographs of the Blue Dragon flow (Figures 13-20) show less textural variation, but a marked variation in color from material near the vent (Figures 13-16) and material near the end of the flow (Figures 17-20). Near the source, the basalt is dark gray, but towards the termination of the flow, the glassy crust is colored an almost purple blue to nearly white pale blue. While observations of texture and color are valuable, it becomes more apparent that vegetation grows preferentially on the smoother pahoehoe slabs. The vegetation would influence the spectra of pahoehoe more than the spectra of a'a or pahoehoe clinker.

Figure 9: Grassy Flow, 7.3 ka, a'a near vent



Figure 10: Grassy Flow, 7.3 ka, a'a near vent, spires rafted to current location



Figure 11: Grassy Flow, 7.3 ka, pahoehoe and flow tube midway along length of flow



Figure 12: Grassy Flow, 7.3 ka, field of small clinker midway along length of flow, next to previous figure



Figure 13: Blue Dragon Flow, 2.1 ka, dark grey pahoehoe and a'a near vent



Figure 14: Blue Dragon Flow, 2.1 ka, pahoehoe with occasional surface color near vent



Figure 15: Blue Dragon Flow, 2.1 ka, pahoehoe near vent, areas of deflation on either side of crack that may overlie a lava tube



Figure 16: Blue Dragon Flow, 2.1 ka, deflation cracks parallel direction of flow near vent



Figure 17: Blue Dragon Flow, 2.1 ka, dark grey pahoehoe with sparse vegetation near termination



Figure 18: Blue Dragon Flow, 2.1 ka, Smooth glassy surface near termination, lava squeezed up through cracks after surface chilled. Vegetation grows preferentially in low spots at edge of squeeze-up.



Figure 19: Blue Dragon Flow, 2.1 ka, fragile colored glassy surface near termination. Pahoehoe flow features preserved under glassy crust. Blue color observed only on glassy surface.

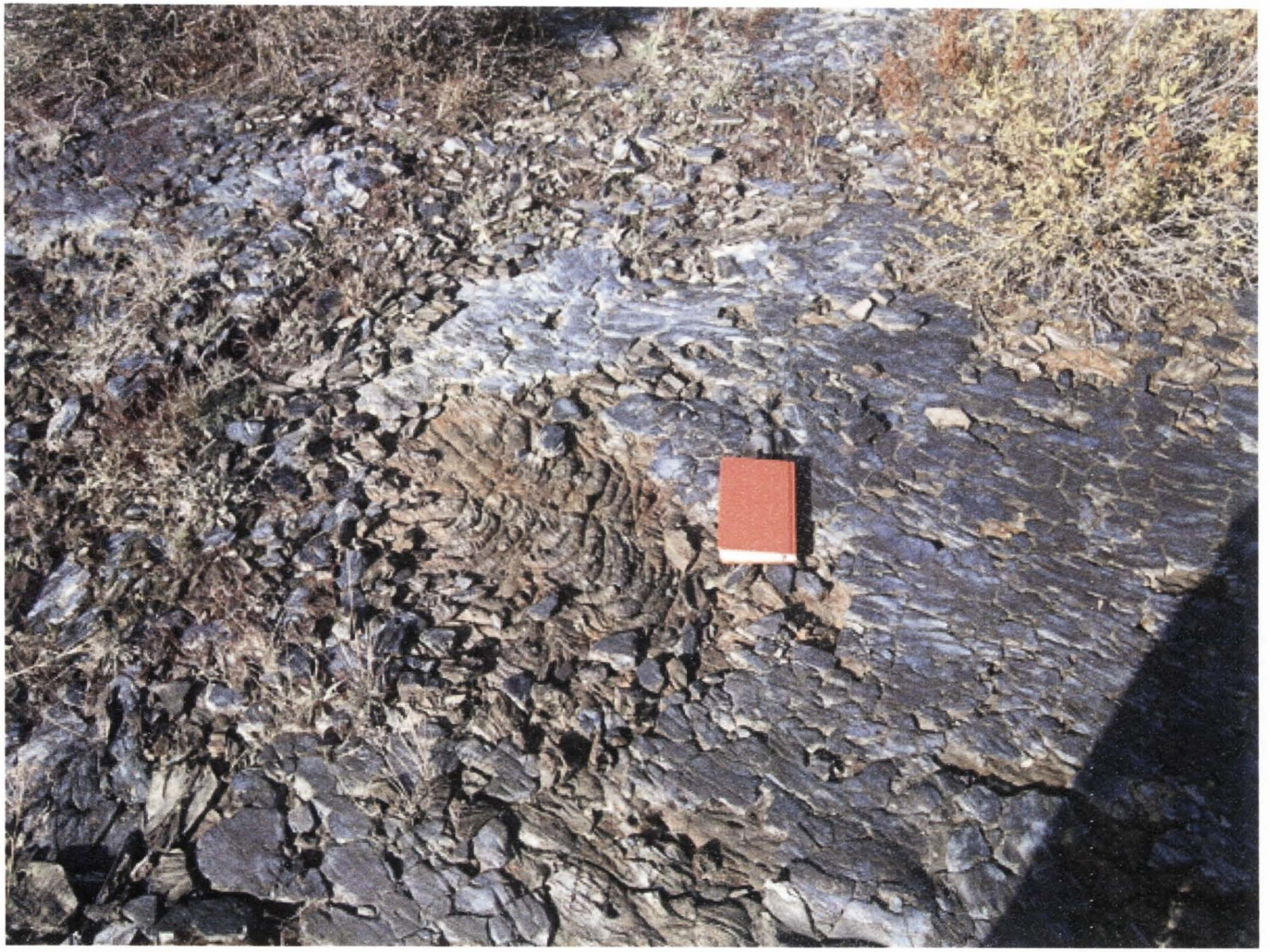


Figure 20: Blue Dragon Flow, 2.1 ka, colored surface of flow near termination. Blue color observed only on glassy surface.



Principal Component Analysis

A principal component analysis of the region of interest was also performed on the isolated basalt (Figure 7). The principal component analysis collects the variation from all the available sensor bands using a linear combination of those bands. The coefficients are determined through statistical analysis of how well correlated the sensor bands are to each other. Once complete, the majority of information contained in all bands can be observed in 2 or 3 of the principal components. Displaying the first 3 principal components as an RGB image allows the analyst to see 99.8% of the variation in the scene simultaneously (Figure 21).

The majority of the spectral variation in the CMNP lava flows comes from the thermal infrared portion of the spectrum (Figure 22). Principal component 2 (Figure 23) comes primarily from bands 5 and 7, possibly indicating minor amounts vegetation or hydrothermal alteration. Together, these two principal components comprise 99.8% of the variation in the Landsat data under the mask. The remaining 0.2% will not likely yield significant results (Figure 24, Table 3).

Figure 21: Principal Component Analysis RGB image of Principal Components 1-3

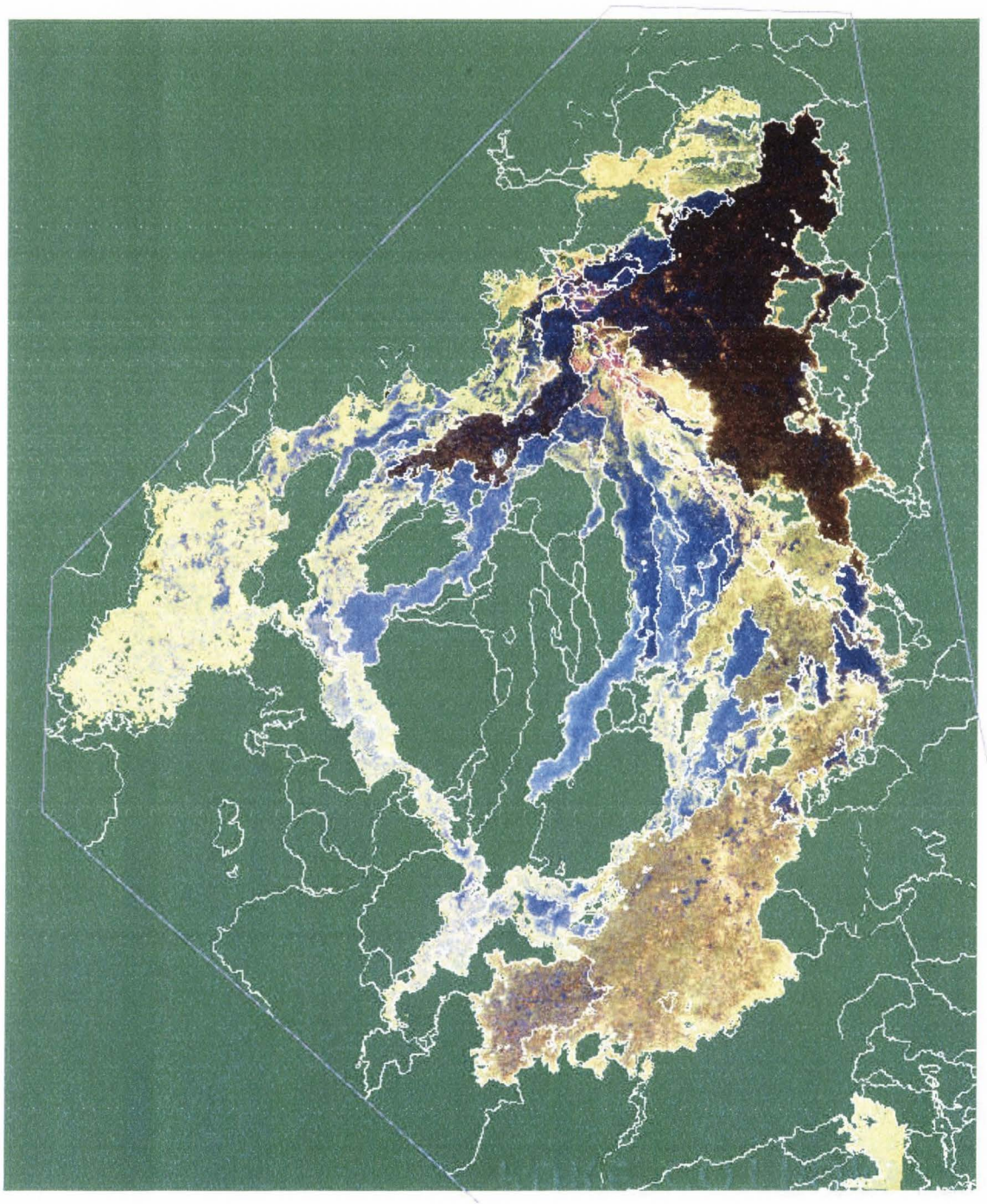


Figure 22: Principal Component 1 (97.694% of Total Variance)

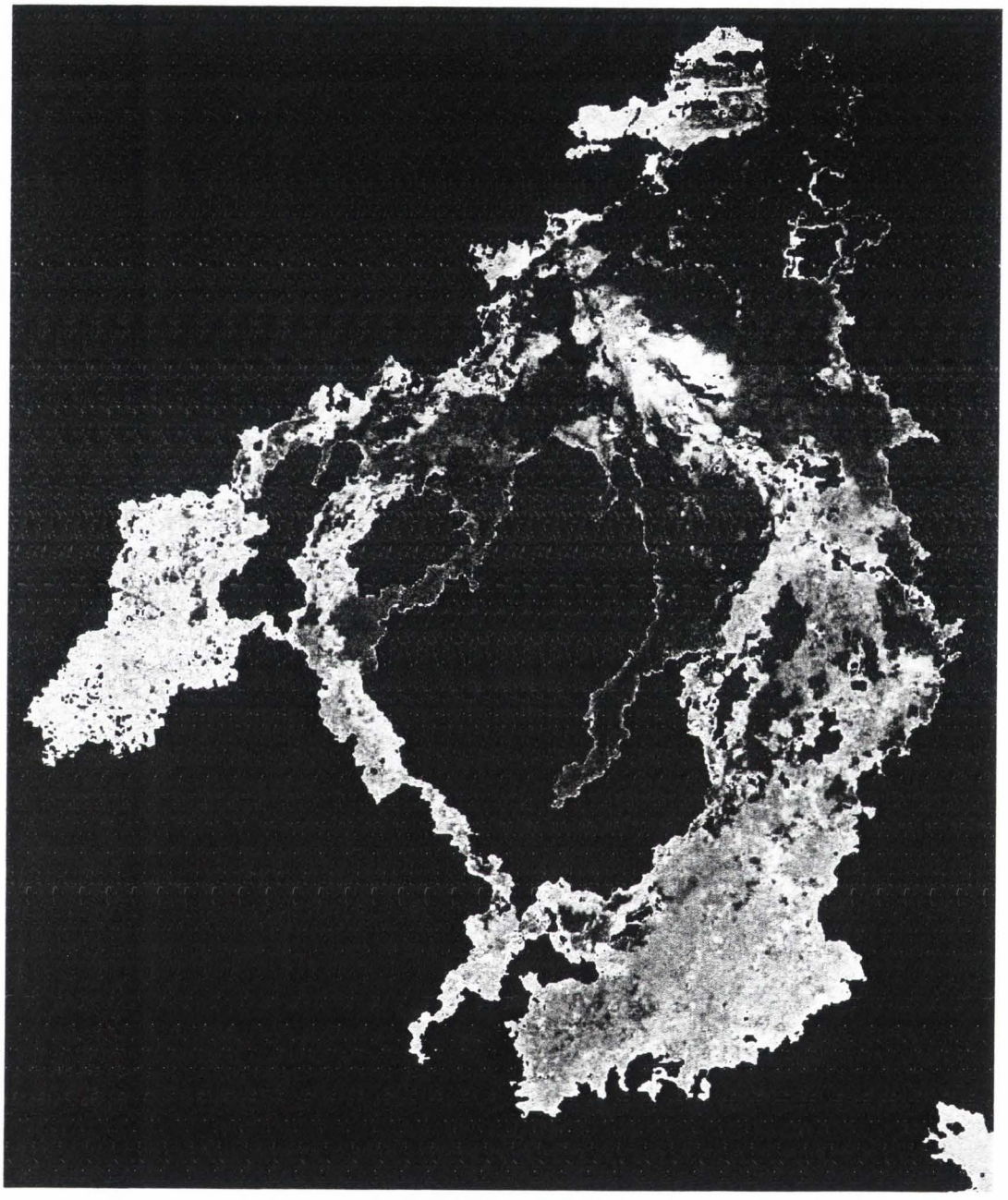


Figure 23: Principal Component 2 (2.147% of Total Variance)

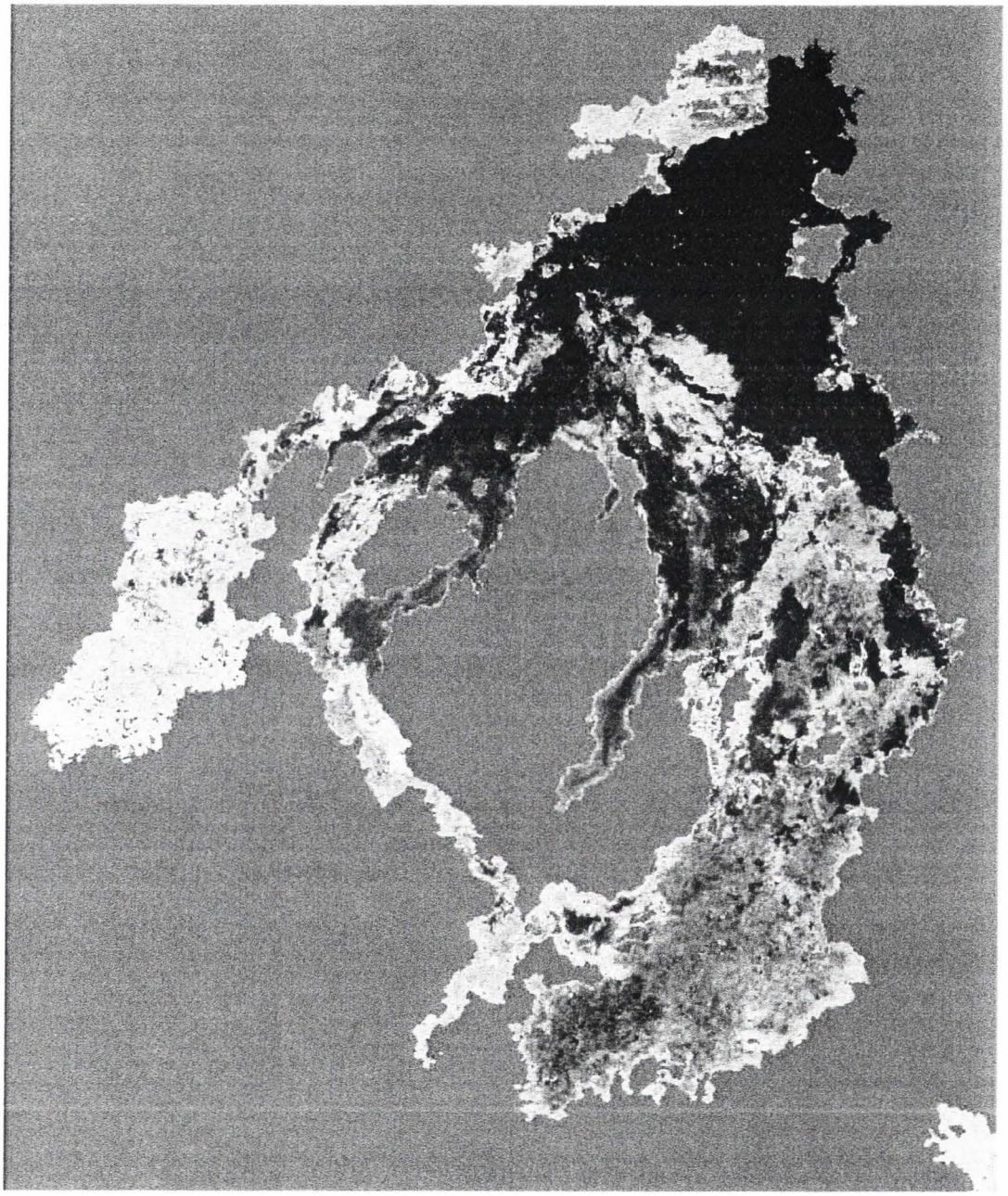


Figure 24: Principal Component 3 (0.126% of Total Variance)

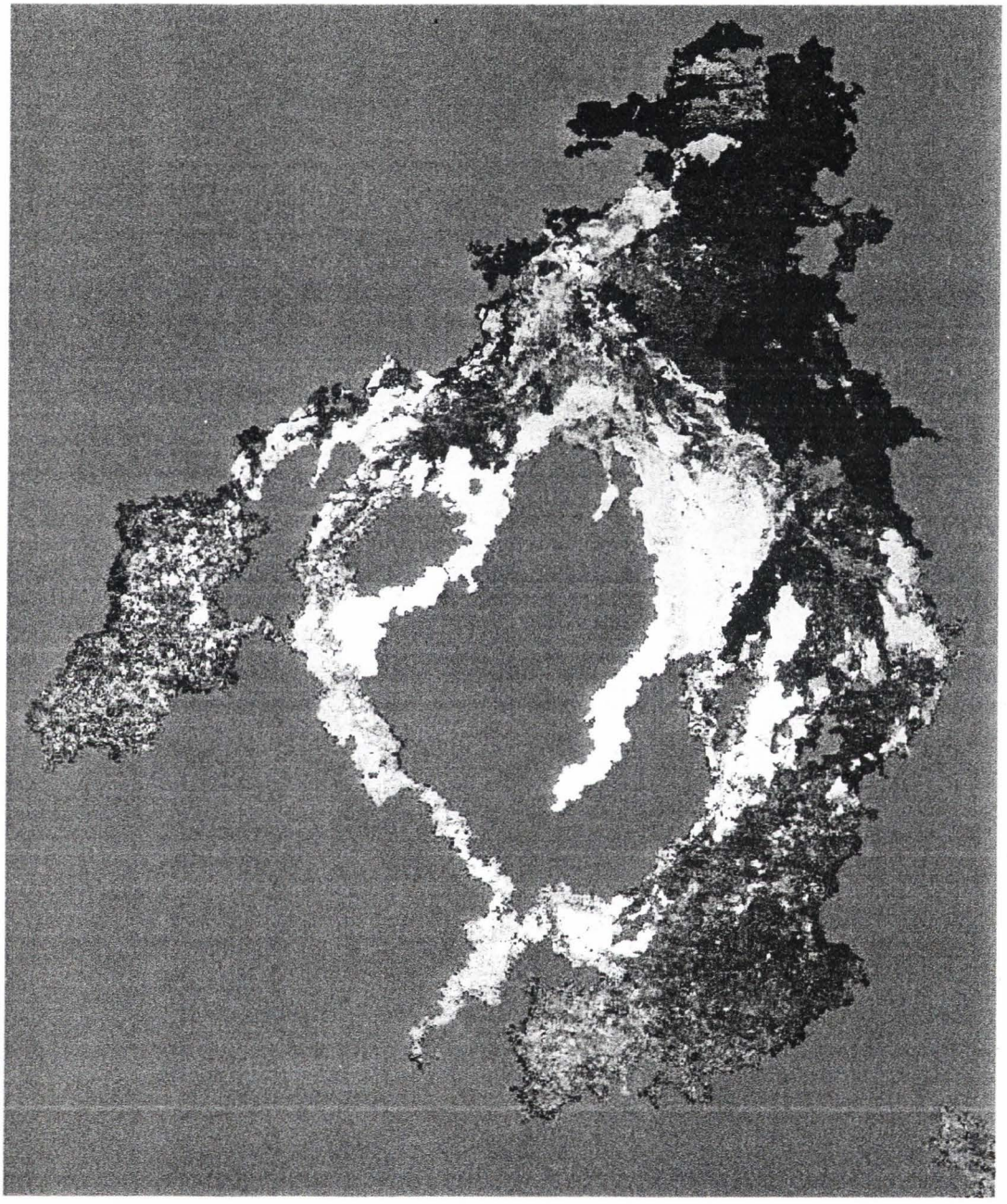


Table 3: Principal Components

PC #	1	2	3	4	5	6	7	
Band 1	0.3770	-0.0510	-0.3739	0.7087	-0.1411	-0.3968	-0.1892	Blue
Band 2	0.1514	0.0295	-0.3474	0.1091	0.0582	0.2170	0.8906	Green
Band 3	0.1788	0.0755	-0.5405	-0.0702	0.3478	0.6149	-0.4077	Red
Band 4	0.1558	0.1874	-0.4962	-0.6468	-0.1494	-0.5035	-0.0146	Near-infrared
Band 5	0.3342	0.7754	0.2319	0.0414	-0.4189	0.2352	-0.0271	Mid-infrared
Band 6	0.7962	-0.4496	0.3138	-0.2421	-0.0023	0.0812	0.0120	Thermal Infrared
Band 7	0.1817	0.3903	0.2209	0.0472	0.8111	-0.3192	0.0614	Thermal Infrared
Variance	10675.015	234.588	13.787	2.081	0.852	0.498	0.203	
	97.694%	2.147%	0.126%	0.019%	0.008%	0.005%	0.002%	
Primary Source	Thermal infrared	Mid-infrared	Mid- to Thermal Infrared	Blue	Thermal Infrared	Red	Green	

Results

The comparison of spectra to geochemistry did not result in a reliable way to determine the chemical composition of a lava flow from the observed spectra. The principal components did not have any discernable correlation to the geochemistry of the lava flows (Figures 25, 26, 27).

One correlation did stand out: The age of a flow displayed a linear relationship to Bands 5 and 7 (both mid-infrared) indicating that the weathering of the lava flows is observable with these bands (Figures 28, 29). In contrast, age did not correlate as well with visible (Bands 1, 2, 3, 8) or thermal infrared (Band 6) bands (Figures 30, 31).

Figure 25: Craters of the Moon Lava Flows, Principal Component 1 vs Geochemistry

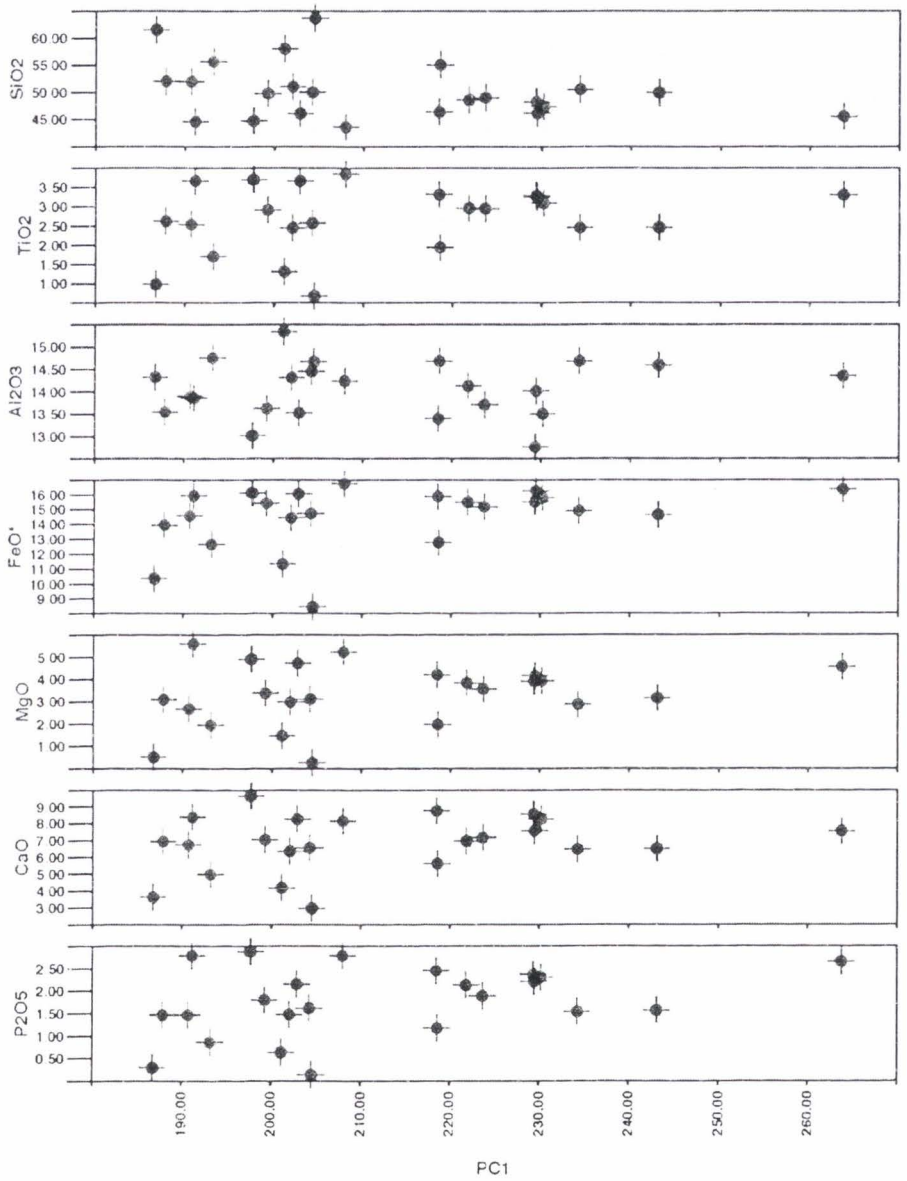


Figure 26: Craters of the Moon Lava Flows, Principal Component 2 vs Geochemistry

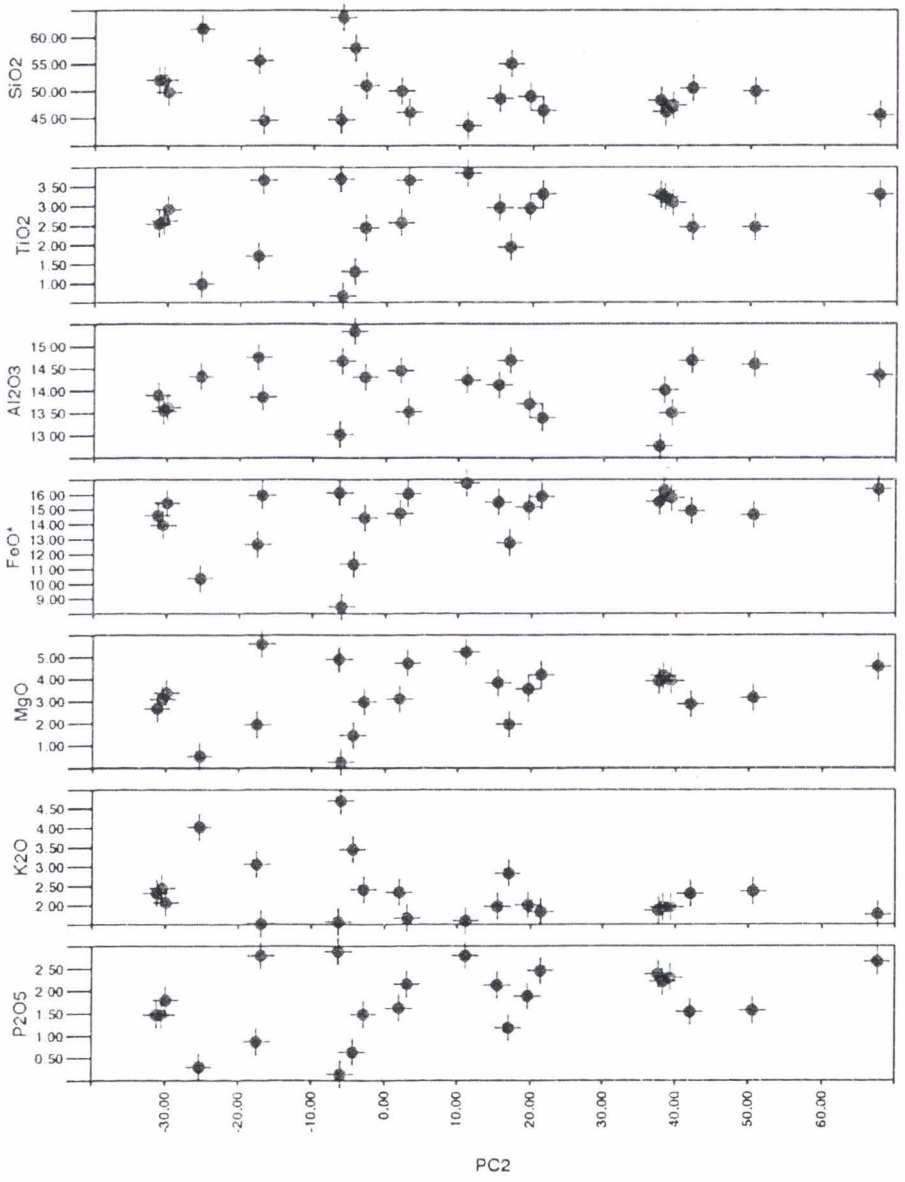


Figure 27: Craters of the Moon Lava Flows, Principal Component 3 vs Geochemistry

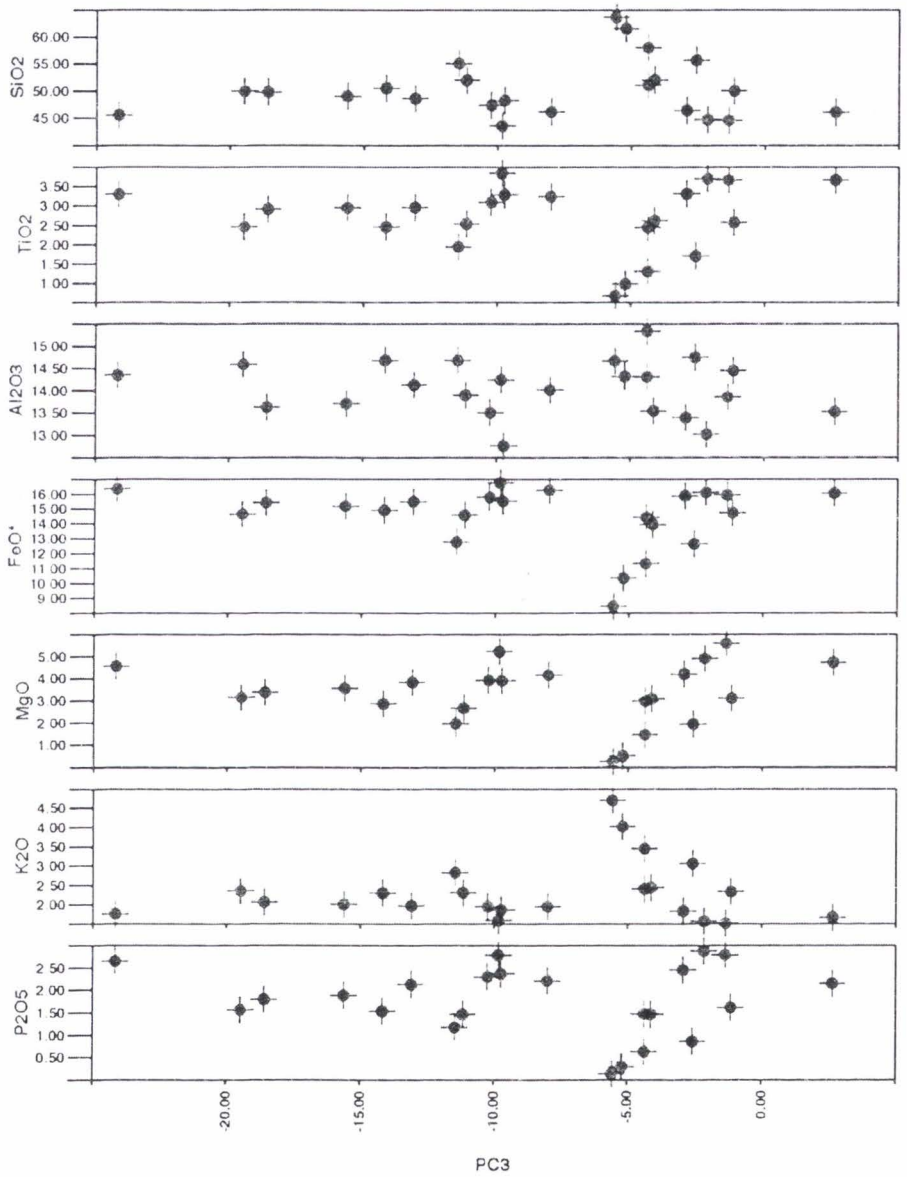


Figure 28: Craters of the Moon Lava Flows, Age vs. Band 7 (Mid-infrared)

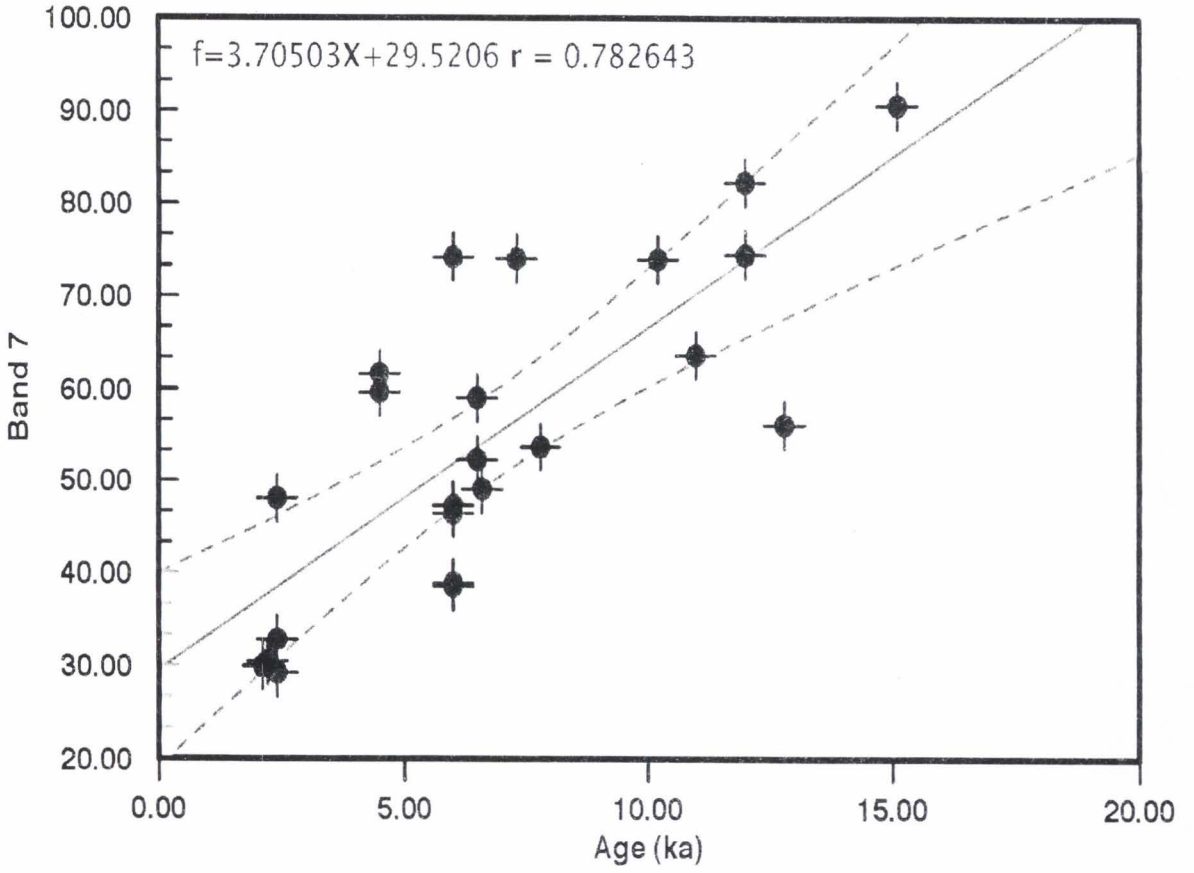


Figure 29: Craters of the Moon Lava Flows, Age vs. Band 5 (Mid-infrared)

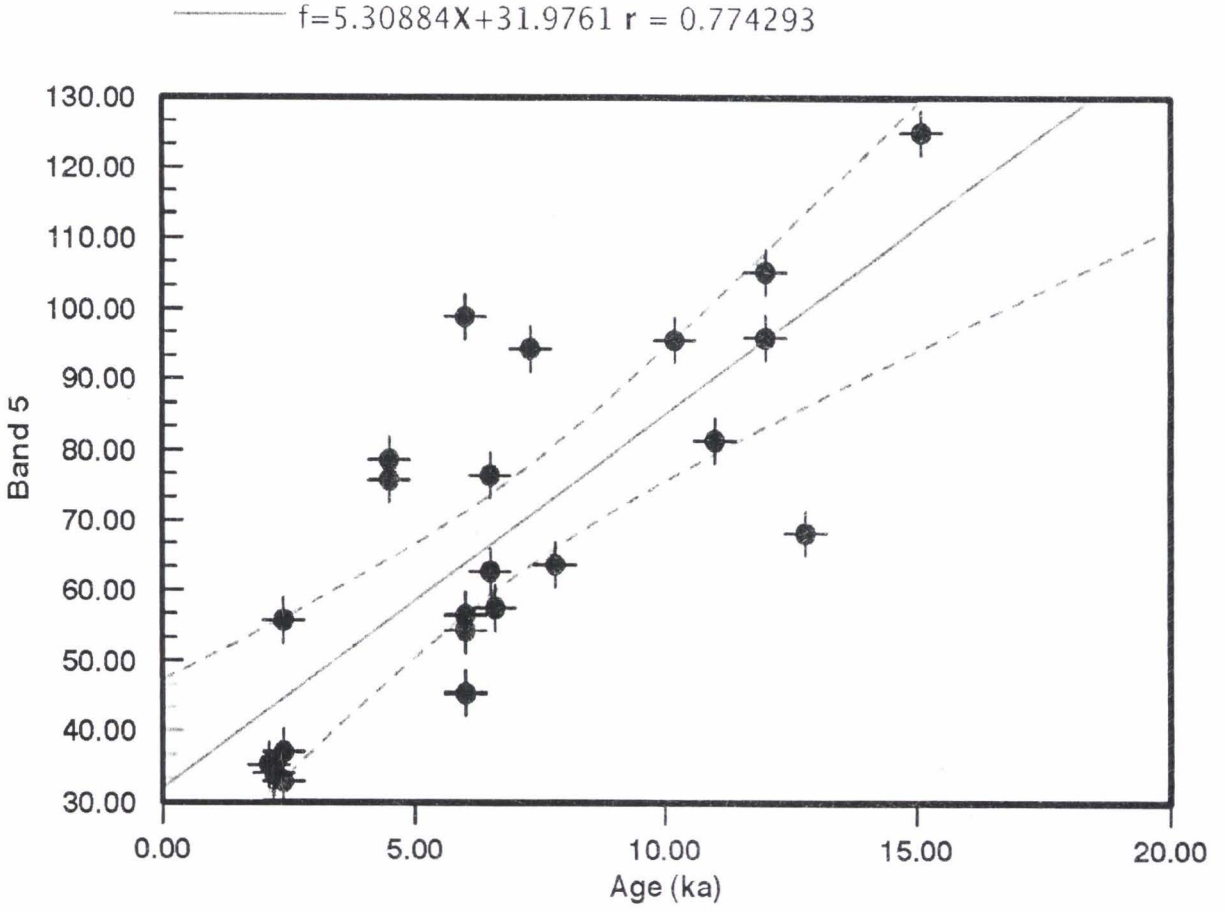


Figure 30: Craters of the Moon Lava Flows, Age vs Band 8 (Panchromatic)

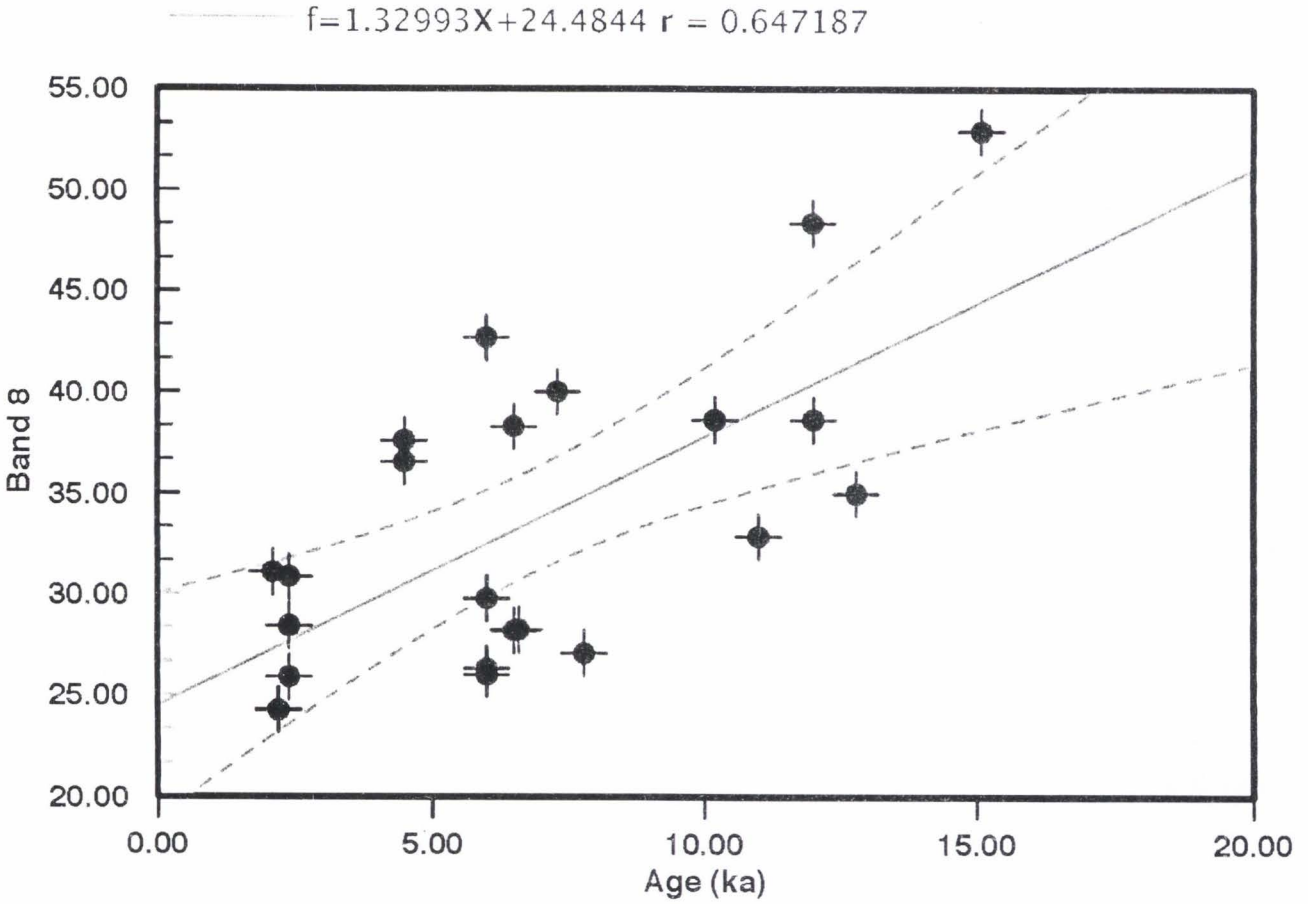
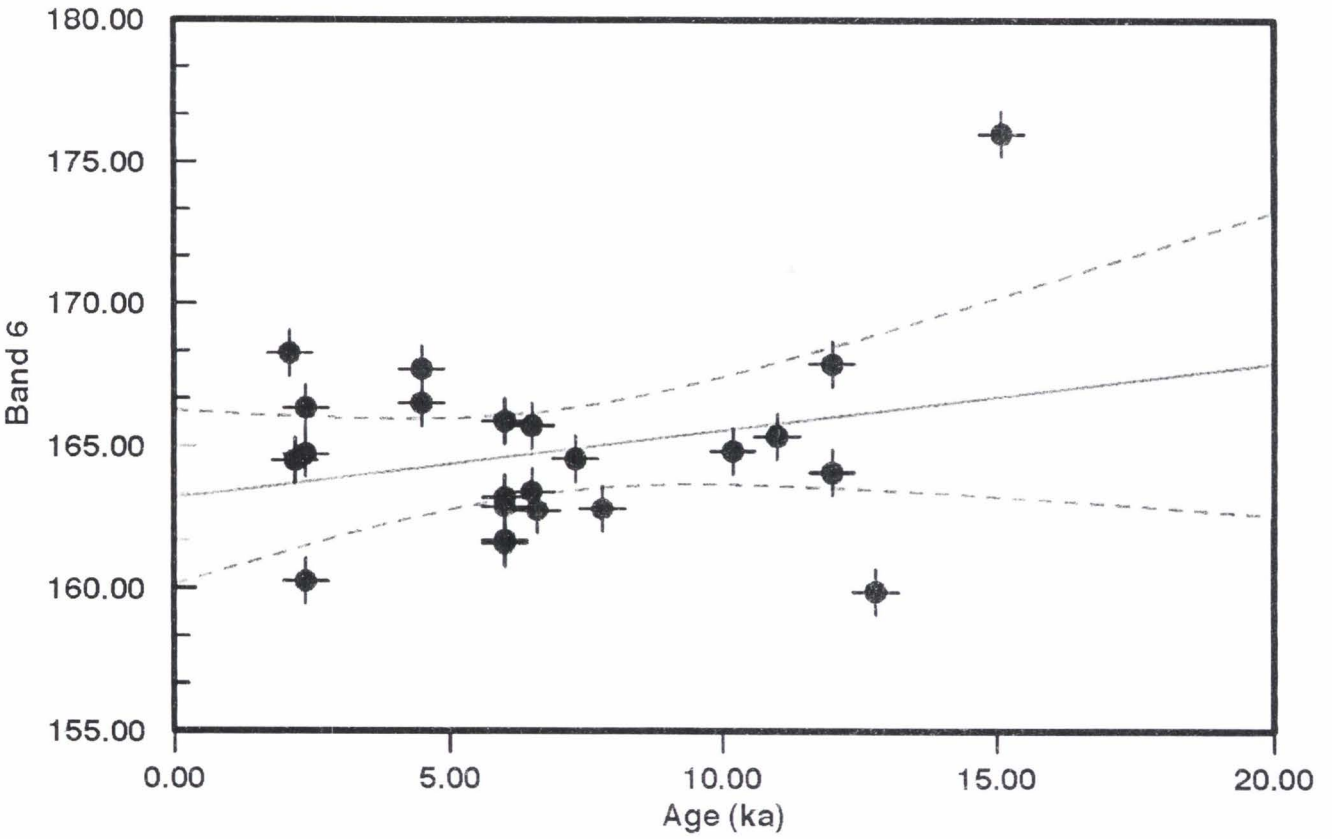


Figure 31: Craters of the Moon Lava Flows, Age vs Band 6 (Thermal infrared)



Field Mapping Twin Falls NE, Hunt, and Eden NE Quadrangles

Fieldwork, conducted in May 2004 and sponsored by the Idaho Geologic Survey, addressed the extent of individual lava flows and effects of the Bonneville Flood. Aerial photographs were examined before and after fieldwork to refine observations. Samples were collected in the field and their location recorded by GPS.

Methods

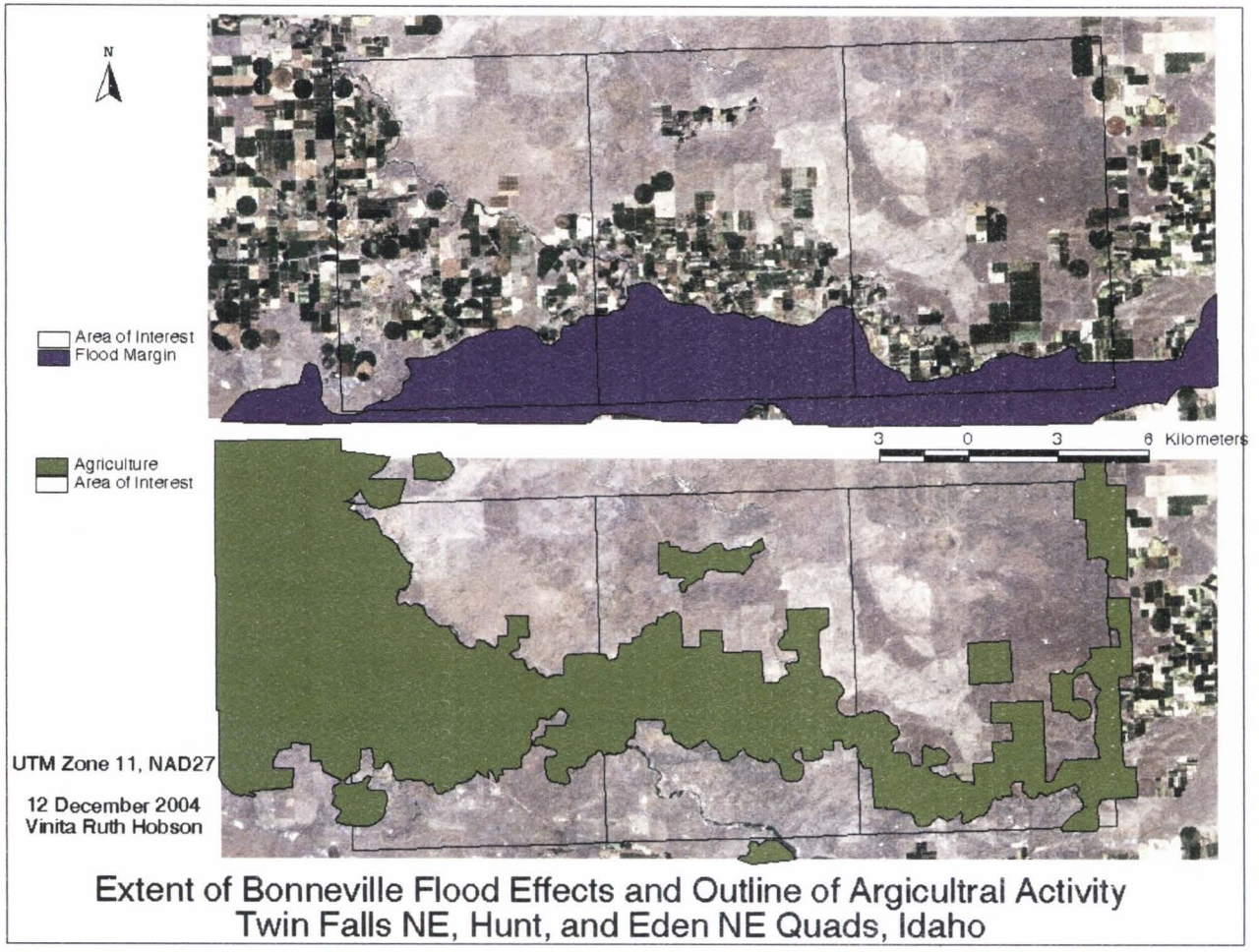
Prior to fieldwork, Digital Orthophoto Quarter Quadrangles (DOQQs) were downloaded from the USGS EROS Data Center and printed to match the USGS 7.5 Minute Topographic Maps 1:24000 scale. Tentative contacts were sketched on the printed images. Landsat ETM data were downloaded from University of Maryland FTP Site. DLG files downloaded from USGS in SDTS format. DEM downloaded from USGS EROS Data Center. Additional aerial photographs for the region of interest and adjoining quadrangles were studied when available.

Fieldwork in May 2004 by Ruth Hobson and Meghan Zarnetske yielded hand samples and Trimble Scoutmaster GPS coordinates for each sample site. Using the sketched tentative contacts as a starting point, observed contacts were sketched on topographic maps.

Following fieldwork, further observations of aerial photograph stereo pairs (at the Idaho Geologic Survey in Moscow, Idaho) were marked in a different color on the printed images. These contacts were field checked in October 2004 and traced onto topographic maps printed in green on heavy Mylar. These derived contacts between geologic units were scanned as tiffs and converted to an ArcView-useable format (BIL – Band Interleaved by Line). The images were registered in ARC using the topographic map corners as tic marks. The images were then rectified to display them with other data in UTM Zone 11, NAD27.

Similar to the geologic contacts, outlines of agricultural activity and the effects of the Bonneville flood were produced from the DOQQs and field notes, creating new polygon themes in ArcView (Figure 32). Observations of flood scouring and flood deposits helped outline the area. These themes were much easier to produce, since they each only had one category in them.

Figure 32:Outlines of Bonneville Flood Effects and Agricultural Activity



Because the loess must be sufficiently thick to run farm machinery without breaking the equipment on subsurface basalt, only 34.81% of the ground in these quadrangles is farmed (Table 4). Much the area that is farmed has had additional soil trucked in from other areas.

The effects of the Bonneville flood include stripping the soil from basalt flows and plucking boulders from the basalt flows themselves. The stripped, scoured and weathered basalt is not conducive to agricultural activities. Agricultural activity indicates that the amount of dirt and soil overlying the basalt layers are sufficiently thick to support these activities. Any attempt to use remote sensing to map the underlying basalt would be impaired by the presence of vegetation, irrigation water and thick soil.

Table 4: Areas affected by Earth-changing Activities

Quad	Quad Area	Agriculture	Agriculture %	Flood	Flood %
Eden NE	142338400	35977700	25.28%	12030600	8.45%
Hunt	142321500	46861900	32.93%	36818800	25.87%
Twin Falls NE	142291500	65762300	46.22%	21842400	15.35%
Total	426951400	148601900	34.81%	70691800	16.56%

Landsat ETM data were downloaded as GeoTiffs in UTM Zone 11, WGS84. Each band came as an individual file. To save repetition of

commands, the bands were layer stacked in ENVI and converted to UTM Zone 11, NAD27. Bands 321 were displayed as RGB to produce a nearly true-color image. The files were then subset to be a little larger than the area of interest.

The DEM was downloaded in four geographic tiles. The four tiles were joined together to form a mosaic in ENVI, then converted to UTM Zone 11, NAD27. The mosaic was converted to a grid file for use in ArcView. The DEM grid was used to make additional layers: shaded relief (Figure 33) and slope (Figure 34).

Figure 33: Shaded Relief of Topography. Exaggerated topography alone does not conclusively identify vent locations.

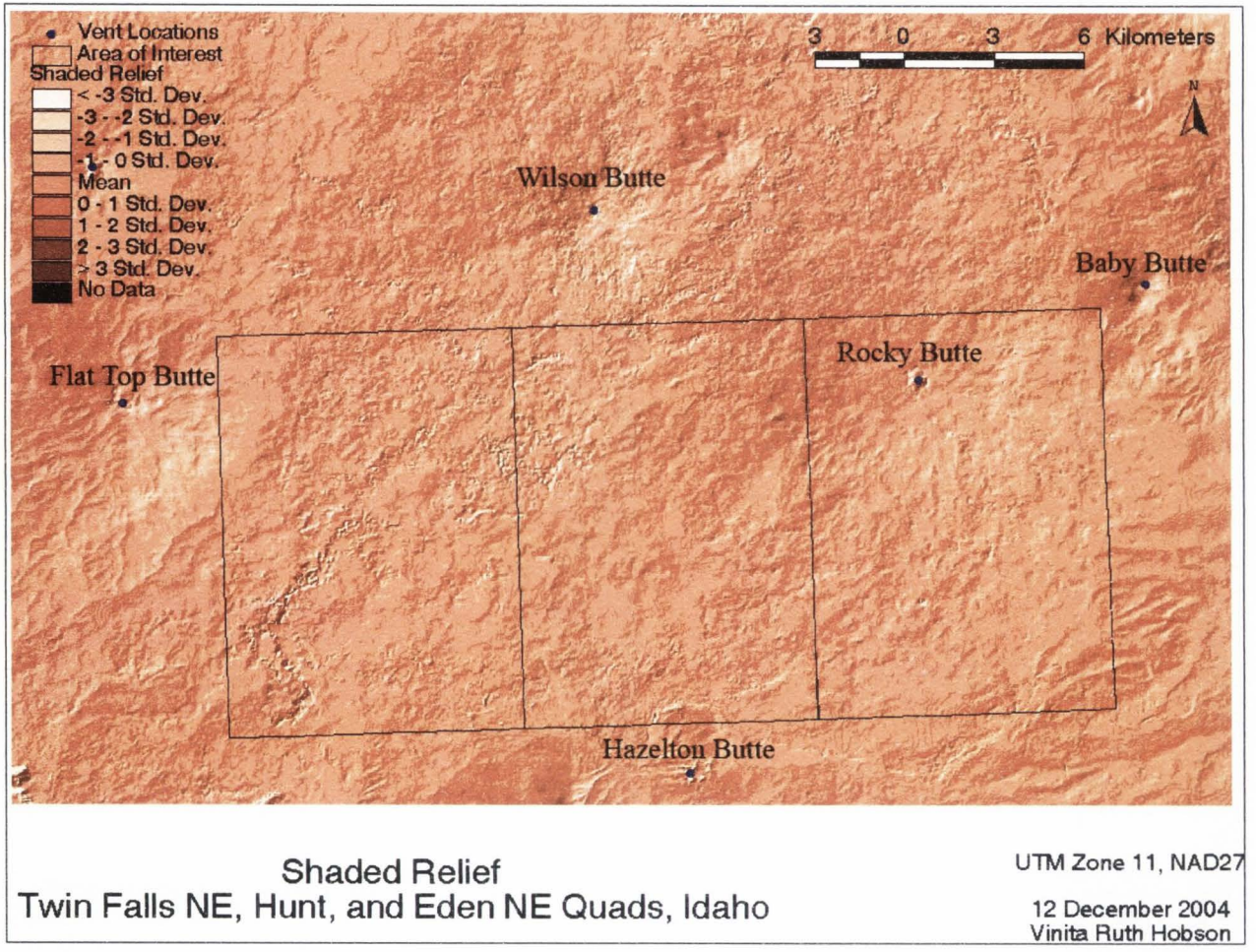
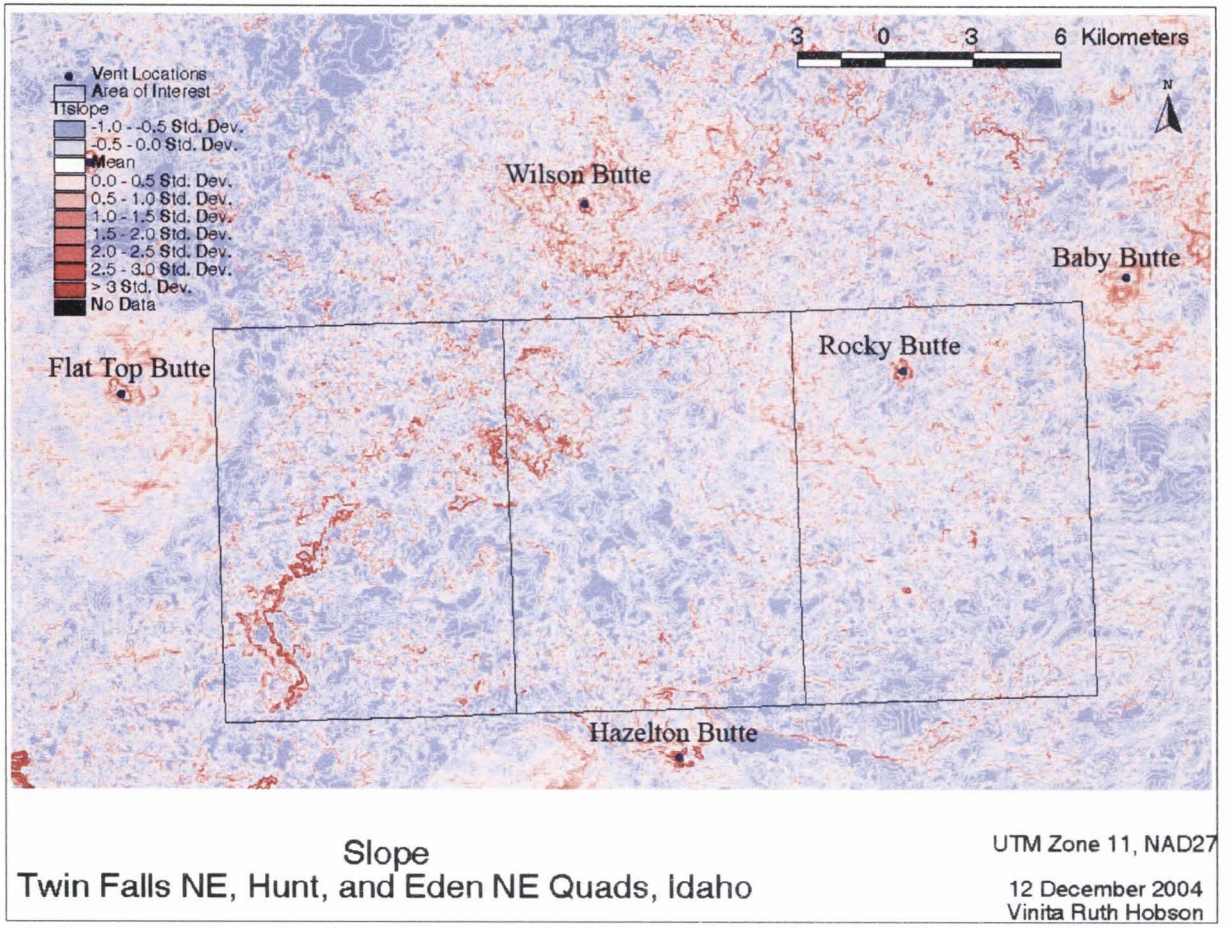


Figure 34: Slope (Rate of change of Elevation) shows distinct rampart features at vent locations. Longer features indicate pronounced edge of flow



Results

Effusive volcanic eruptions bring lava to the surface of the earth. The viscosity of the lava varies depending on chemical composition and temperature. Many of the basalts erupted in the Snake River Plain have a very similar chemical composition (olivine tholeite). Not surprisingly, many of the lava flow characteristics are similar to each other as well. Many of the vents in the area are shield volcanoes, built from many thin, runny lava flows that travel far from the source. Many of the flows have a very shallow overall slope of 5 degrees, very long compared to their thickness. Temperature plays a major role in the behavior of lava. As the lava cools, it becomes increasingly viscous and forms a glassy crust. If the eruption continues, lobe inflates and enough pressure can build to rupture the glassy crust, generating another lobe. This process repeats multiple times with lava flowing through the series of lobes, insulated by the glassy crust that was left in place. When the eruption ceases, the erupted lava flows downhill until it cools enough to solidify. The inflated lobes left behind may slowly collapse or remain as a tube if the walls and roof are strong enough. A channel discovered in a lobe of the Wilson Flow may have transported large volumes of basalt toward the Snake River channel (Figure 35). The geologic units in the Twin Falls NE, Hunt, and Eden NE quadrangles (Figure 36) are labeled according to the vent source.

The loess-covered and much older vents remain in a unit together because they were difficult to distinguish.

Figure 35: Twin Falls NE DOQ and Geologic Contacts

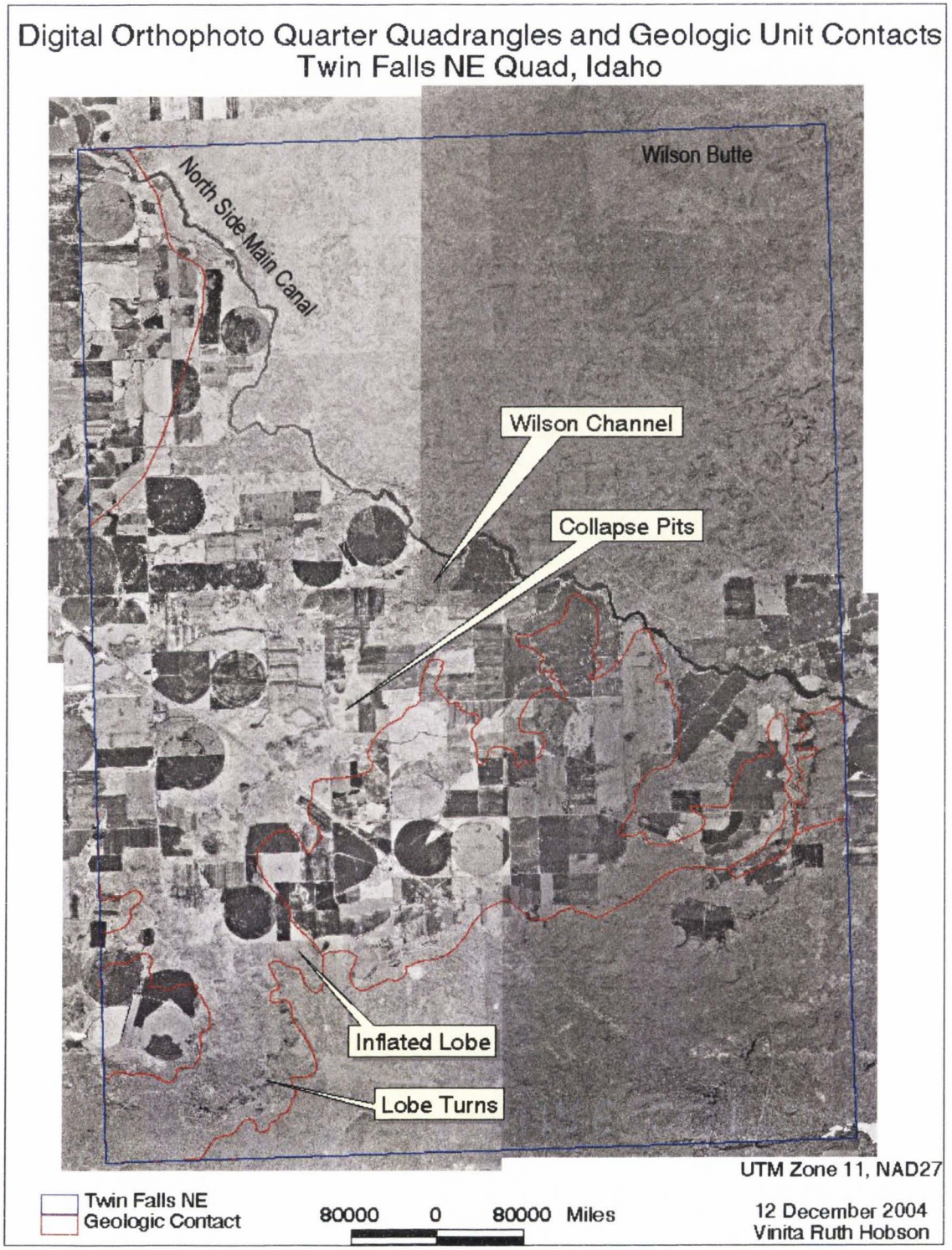
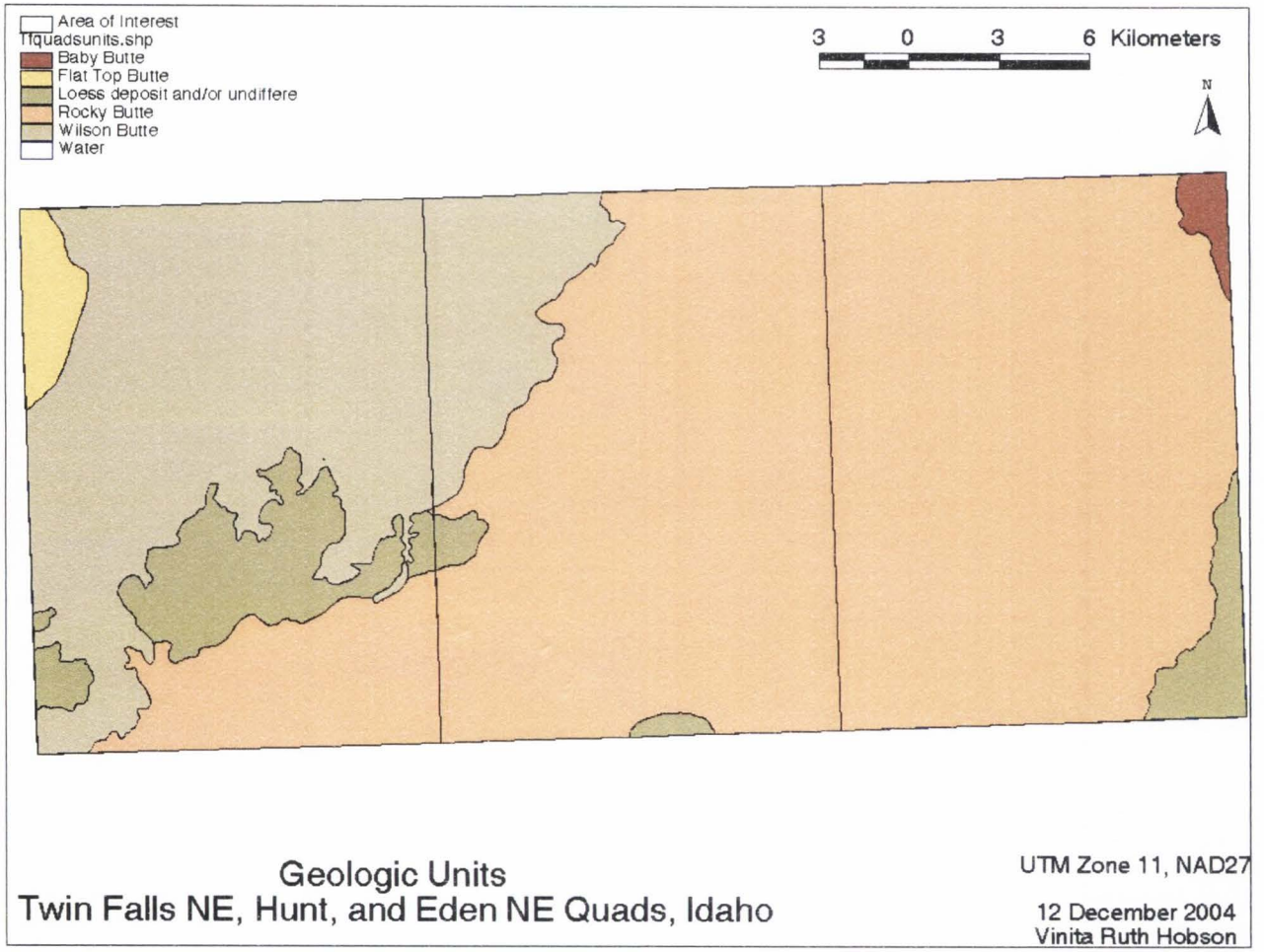


Figure 36: Geologic Units in Twin Falls NE, Hunt, and Eden NE Quadrangles



Conclusions

The various methods of examining phenomena in the Snake River Plain are challenging. Unsupervised classification indicates that the spectra are related to the individual components of flows. However, the comparison of spectra to the geochemical analysis performed by Kuntz et al. (1992) indicates that the chemical components are not strongly correlated to the bands observed with Landsat ETM. Photographs of the flows near Craters of the Moon National Monument show wide variations in texture and color within a single flow. One flow had a'a spires near a vent, but transitioned to pahoehoe and clinker farther away. Another flow's basalt is dark gray near the source, but changes to an almost purple blue and nearly white pale blue-colored glassy crust towards the termination of the flow. While observations of texture and color are valuable, it becomes more apparent that vegetation grows preferentially on the smoother pahoehoe slabs. The vegetation would influence the spectra of pahoehoe more than the spectra of a'a or pahoehoe clinker. Because of the influence of vegetation on the spectra observed, additional vegetation would prohibit using Landsat ETM to map lava flows reliably. Remote sensing reveals some information about the texture and color of lava flows, but attempts to map flows where there is more ground cover are overwhelmed by the contribution of vegetation. The

significant differences in vegetation and soil cover require that different methods be used to map flows in this region.

Elevation data reveal the locations of the ramparts at the source vent, but do not define the edge of a flow. Field observations of terrain in combination with geochemical analysis of samples collected by previous graduate students is more reliable in defining the flows and which source vent they emerged from than remote sensing using Landsat ETM.

References

Camp, V. E., 1995, Mid-Miocene propagation of the Yellowstone mantle plume head beneath the Columbia River basalt source region: Geology, v. 23, no. 5, p. 435-438.

Christiansen, R. L., Foulger, G. R. and Evans, J. R., 2002, Upper-mantle origin of the Yellowstone hotspot: Geological Society of America Bulletin, v. 114, no. 10, P. 1245-1256.

Geist, D. and Richards, M., 1993, Origin of the Columbia Plateau and Snake River Plain: Deflection of the Yellowstone plume: Geology, v. 21, p. 789-792.

Hackett, B. and Bonnichsen, B., 1994, Volcanic Crescent *in* Shallat, T, ed., Snake: The Plain and Its People: Boise, Idaho, Boise State University, p. 25-53.

Hill, R. I., 1991, Starting plumes and continental break-up: Earth and Planetary Science Letters, v. 104, p. 398-416.

Humphreys, E. D., Dueker, K. G., Schutt, D. L. and Smith, R. B., 2000, Beneath Yellowstone: Evaluating Plume and Nonplume Models Using Teleseismic Images of the Upper Mantle: GSA Today, v. 10, no. 12, p. 1-7.

Kuntz, M. E., Champion, D. E., Lefebrve, R. H. and Covington, H. R., 1988, Geologic Map of the Craters of the Moon, Kings Bowl, and Wapi Lava Fields, and the Great Rift Volcanic Zone, South-central Idaho, U. S. Geological Survey Miscellaneous Investigations Series Map I-1632, Scale 1:100,00, 1 sheet.

Kuntz, M. A., Champion, D. E., Spiker, E. C., Lefebvre, R. H. and McBroome, L. A., 1982, The Great Rift and the Evolution of Craters of the Moon Lava Field, Idaho, *in* Bonnichsen, B. and Breckenridge, R. M., eds., Cenozoic Geology of Idaho: Idaho Bureau of Mines and Geology Bulletin 26, p. 423-437.

Kuntz, M. A., Covington, H. R. and Schorr, L. J., 1992. An Overview of basaltic volcanism of the eastern Snake River Plain, Idaho, Chapter 12 *in* Link, PK, MA Kuntz, and LB Platt, eds., Regional Geology of Eastern Idaho and Western Wyoming: Geological Society of America Memoir 179, p. 227-267.

Lefebvre, R. H., 1975, Mapping in the Craters of the Moon volcanic field, Idaho, with Landsat (ERTS) imagery, *in* Proceedings of the International Symposium on Remote Sensing of Environment 10, v. 2: Ann Arbor, University of Michigan, p. 951-957.

Peng, X. and Humphreys, E. D., 1998, Crustal velocity structure across the eastern Snake River Plain and Yellowstone swell: Journal of Geophysical Research, v. 103, no. B4, p. 7171-7186.

Pierce, K. L. and Morgan, L. A., 1992, The track of the Yellowstone hotspot: Volcanism, faulting, and uplift *in* Link, P. K., Kuntz, M. A., and Platt, L. B., eds., Regional Geology of Eastern Idaho and Western Wyoming: Geological Society of America Memoir 179, p. 1-53.

Saltzer, R. L. and Humphreys, E. D., 1997, Upper mantle P wave velocity structure of the eastern Snake River Plain and its relationship to geodynamic models of the region: Journal of Geophysical Research, v. 102, no. B6, p. 11829-11841.

Schaber, G. G., Elachi, C. and Farr, T. G., 1980. Remote Sensing of SP Mountain and the SP Lava Flow in North-Central Arizona: Remote Sensing of Environment, v. 9, p. 149-170.